Inter-decadal modulations in ENSO teleconnection to northwest Pacific region: Role of the tropical Indian Ocean

J. S. Chowdary[1,2]

Shang-Ping-Xie[2], Hiroki Tokinaga[2], Yuko M. Okumura[3], Hisayuki Kubota[4], Nat Johnson[2] , Xiaotong Zheng[5]

[1] Indian Institute of Tropical Meteorology, India
[2] International Pacific Research Center, University of Hawaii at Manoa, Honolulu, Hawaii
[3] National Center for Atmospheric Research Boulder, Colorado, USA
[4] Japan Agency for Marine-Earth Science and Technology, Yokosuka, Japan
[5] Physical Oceanography Laboratory, Ocean University of China, Qingdao, China

ICTP
Workshop on Variability in the Western Tropical Pacific: Mechanisms, Teleconnections and Impacts on Sub-Seasonal, Inter-Annual and Inter-Decadal Time Scales.
Trieste - Italy, 12 - 16 November 2012

Outline

- Background
- (I) Modulation in ENSO teleconnections to NW Pacific: role of the TIO
- (II) Impact of Indian Ocean SST in predicting NW Pacific summer climate.

Background and motivation

✓Convective activities over the NW Paficic region [100E to 180E and Equator to 40N] and display pronounced interannual variability and has significant impacts on the climate over East Asia (e.g., Nitta, 1987, 1989; Harrison and Larkin 1996; Wang et al. 2000, 2003) and Indian summer monsoon (Chowdary et al 2012 a,b).

✓El Niño – Southern Oscillation (ENSO) has been recognized as the primary factor that determines the interannual variability of the summer climate over the NW Pacific and East Asia (e.g. Wang et al. 2000, 2003; Watanabe and Jin 2002, Xie et al. 2009, 2010).

✓Precipitation (low level circulation) anomalies over the NW Pacific tend to be positive (cyclonic) during El Niño developing years and negative during El Niño decaying (anti-cyclonic) years (Wang et al. 2000, Chou et al., 2003, Xie et al. 2009).

✓During spring (MAM(1)) after peak phase of El Niño, low level circulation or SLP high is well correlated with (negative) local SST anomalies, suggesting a local ocean–atmosphere interaction (Wang et al. 2000; Lau and Nath 2003) and with central Pacific SSTs.

MAM(1) correlation with NDJ(0) Nino-3.4 SST Index (Xie et al., 2009)

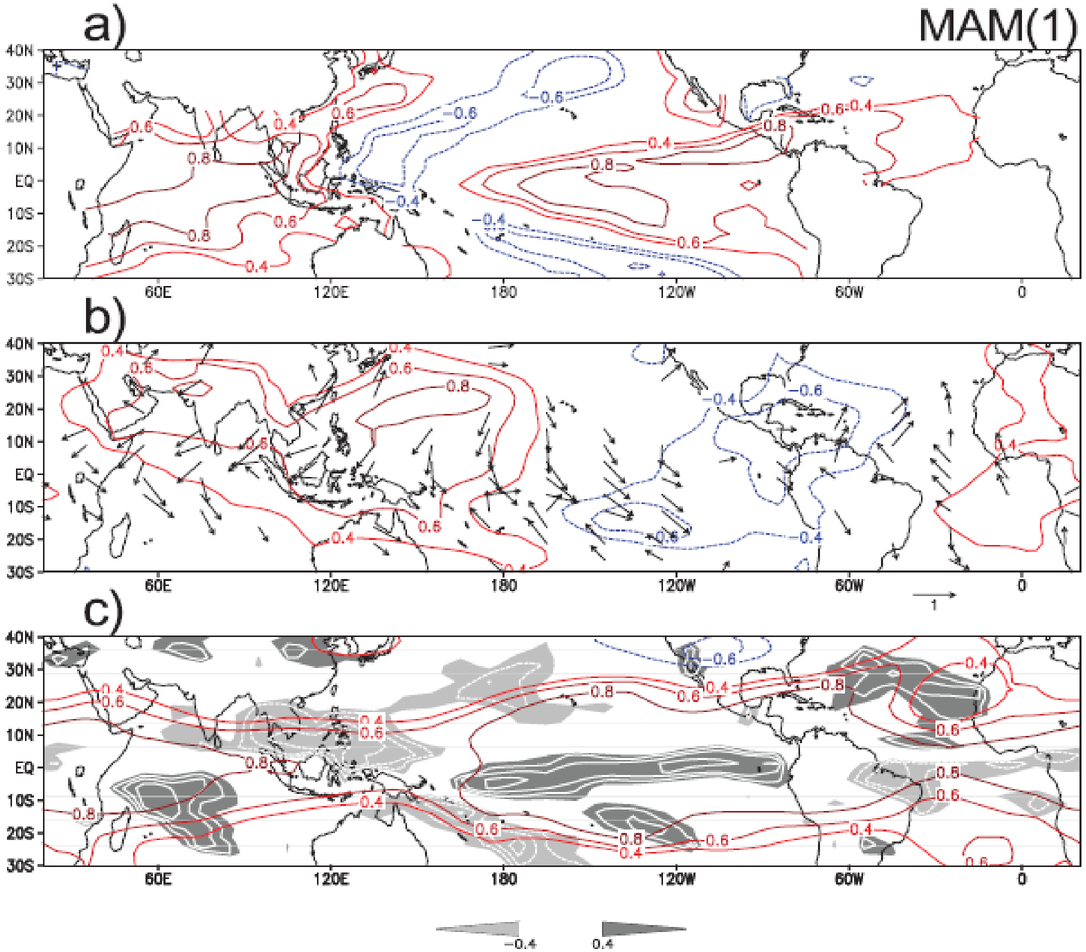

SST

SLP & Winds

Rainfall & TT

The anomalous Philippine Sea anticyclone results from a Rossby-wave response to suppressed convective heating, which is induced by both the in situ ocean surface cooling and the subsidence forced remotely by the central Pacific warming (Wang et al., 2000).

✓NW Pacific low level circulation/rainfall is not correlated with local SST anomalies during summer.

✓Highest SST correlation in North Indian Ocean & South China Sea, not in Pacific

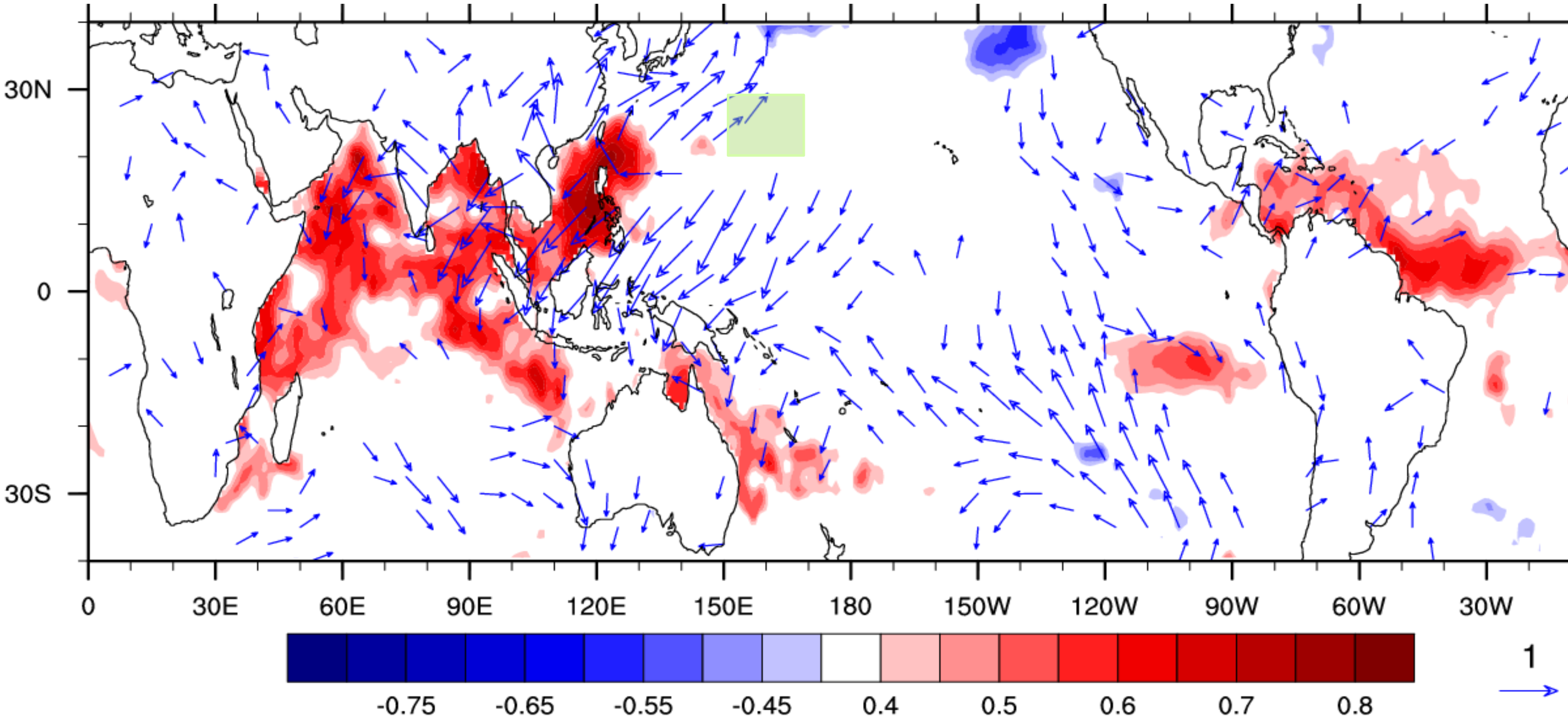

JJA SST & surface wind correlation with the NWP monsoon index of Wang et al. (2001, JC) based on meridional shear

Courtesy of Xia Qu (IAP/CAS) and S-P. Xie (IPRC)

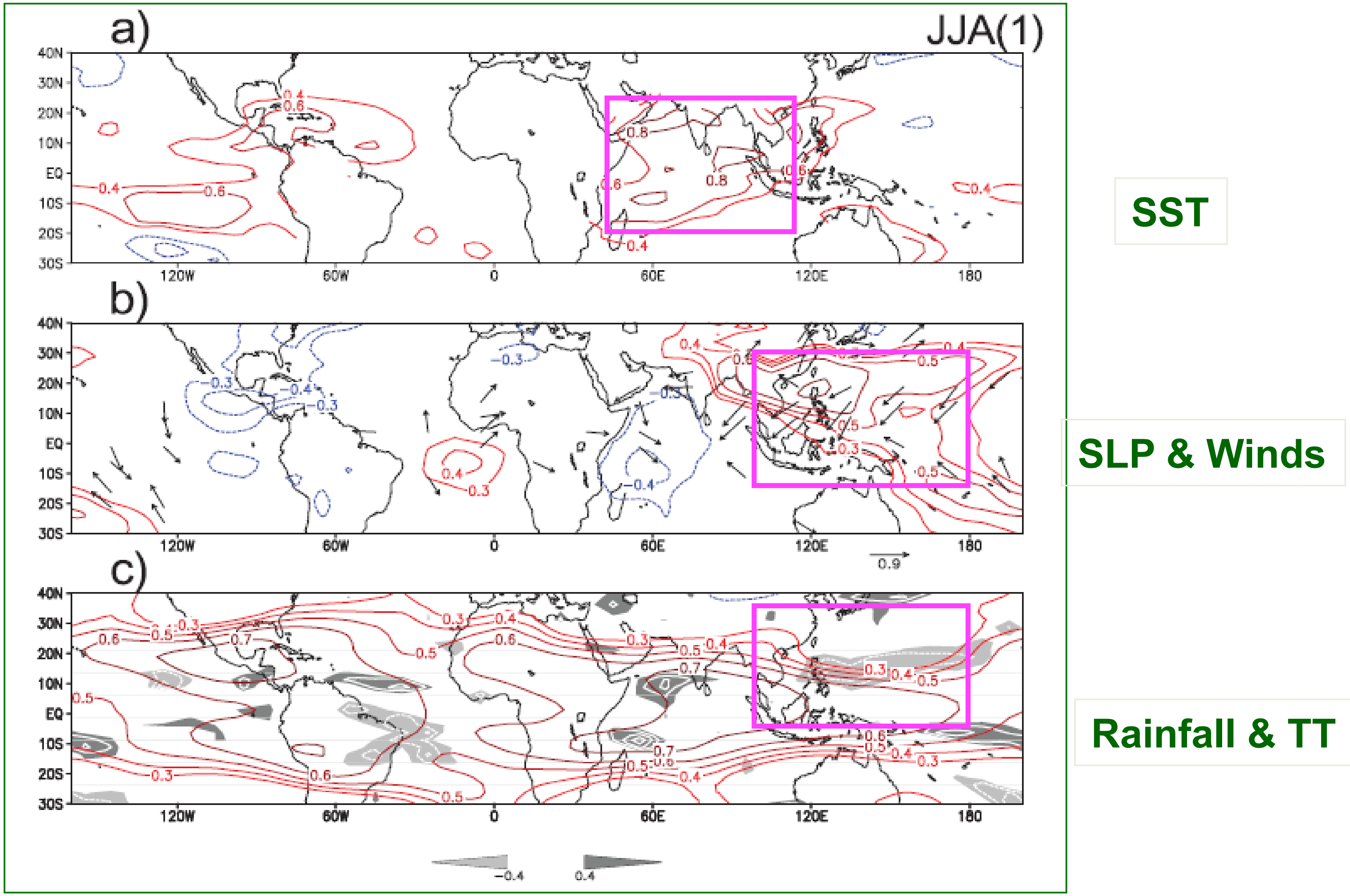

JJA(1) correlation with NDJ(0/1) Nino-3.4 SST Index (Xie at al., 2009)

Walker circulation changes induced by SST anomalies over central-eastern Pacific lead to the decrease of net heat flux from ocean to atmosphere over Indian Ocean. Thus warm SST anomalies occurs around peak phase of NINO SST peaks. (Allan et al. 1995 Klein et al. 1999; Reason et al. 2000; Alexander et al. 2002).

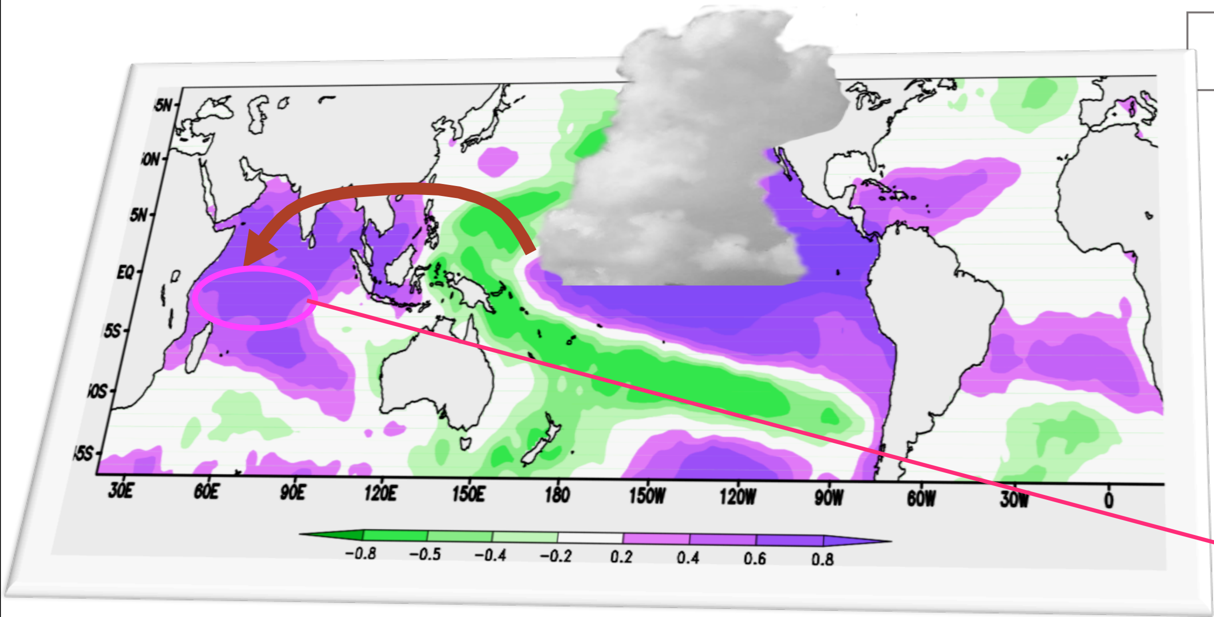

TIO Basin-Mode warming

Atmospheric bridge

The relationship between SST over tropical Southwestern IO and heat flux is not close. The warming is induced by ocean wave dynamics (Xie et al. 2002).

- IO SST warming has long been dismissed as passive on the ground that rainfall decreases there at the peak of El Nino.
- Does IO remain passive in the subsequent seasons?

How do these ENSO-TIO basin-wide warming and NW Pacific circulation are related?

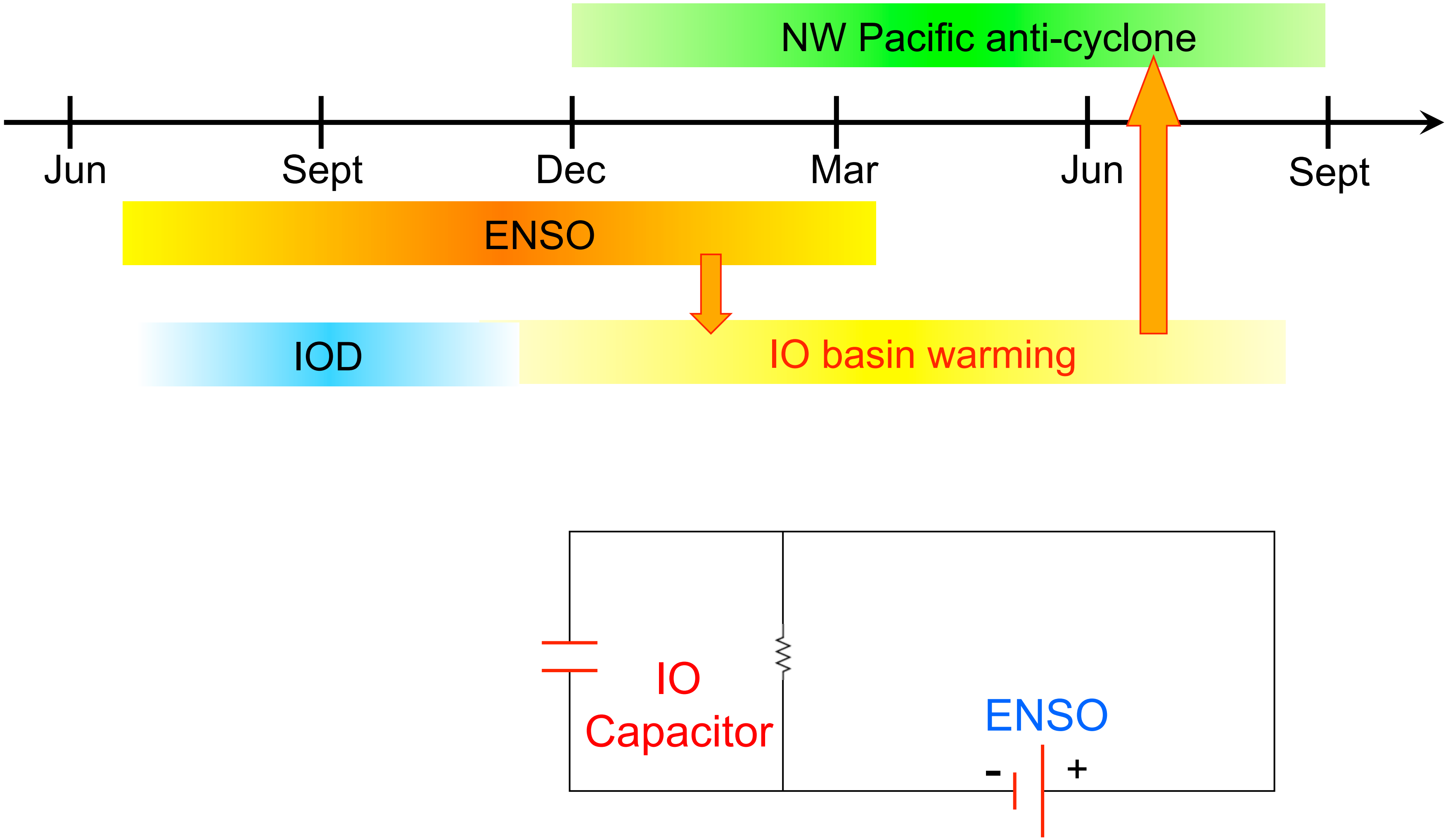

Courtesy of S-P. Xie (IPRC), Xie et al. (2009).

Summer TIO-NW Pacific teleconnections are not constant in time.
Xie et al. 2010; Huang et al. 2010

Correlation with NDJ Nino 3.4.

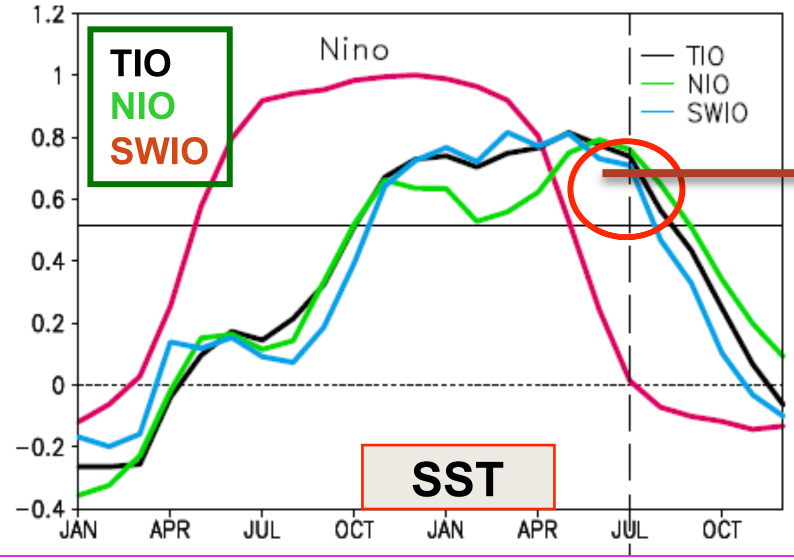

JJA(1) warming

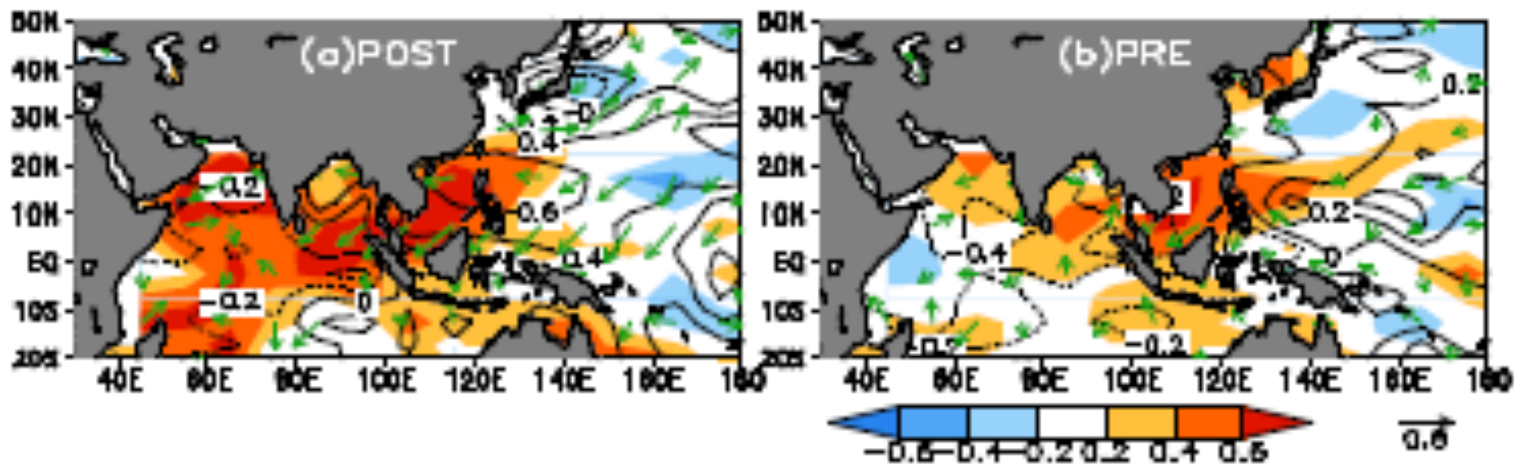

NDJ(0/1) NINO.34 correlation with TIO SST (shaded), Surface winds (vectors) and SLP (contours) before (1950-1976) and after (1977-2006) the 1976 climate shift.

Research into interannual variability over tropical oceans is generally limited to the period after 1950 because of insufficient observational data. The availability of data, however, improves markedly along busy shipping lanes.

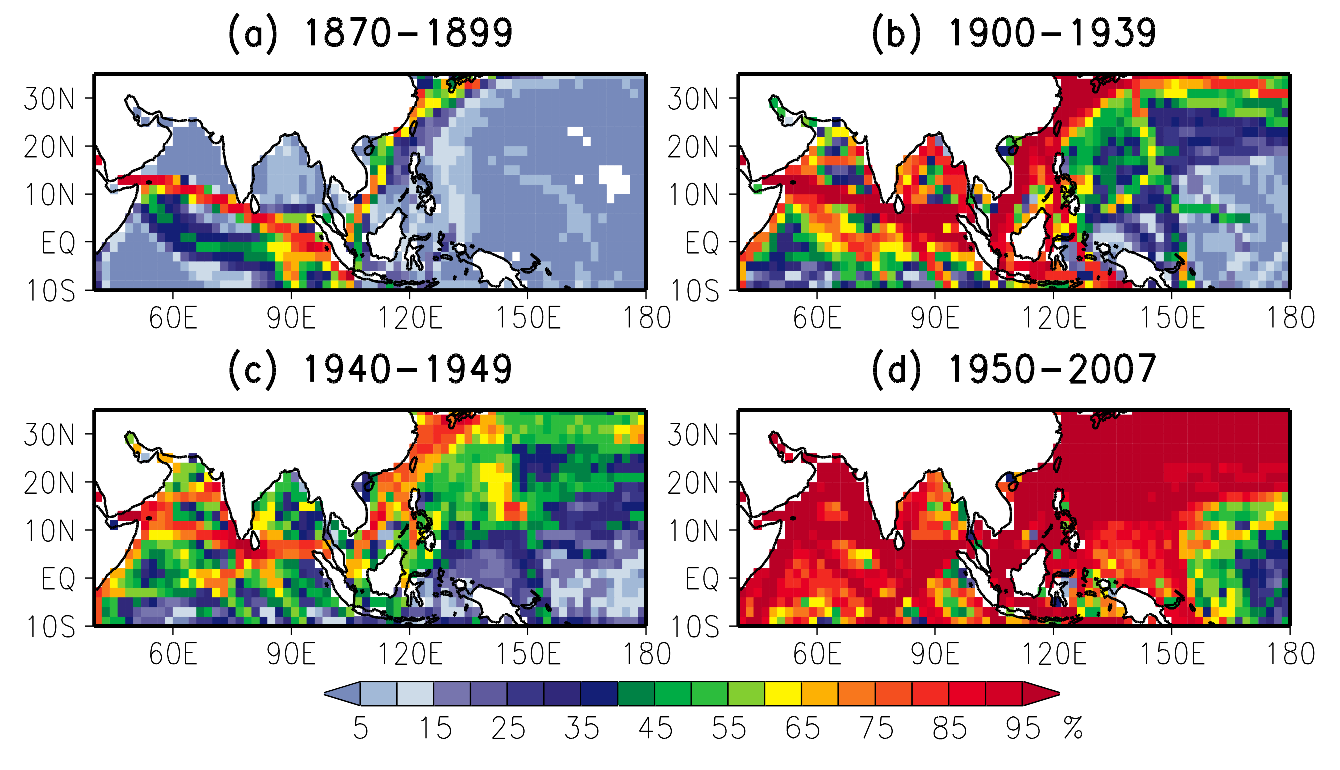

By using ship-board surface meteorological observations along a frequently travelled track across the North Indian Ocean (NIO; from the Gulf of Eden through Malacca Strait), the South China Sea (SCS; to Luzon Strait), and NW Pacific the present study investigates slow modulation of interannual variability along the ship track and its relationship to El Niño/Southern Oscillation (ENSO) for the period from 1870-2007.

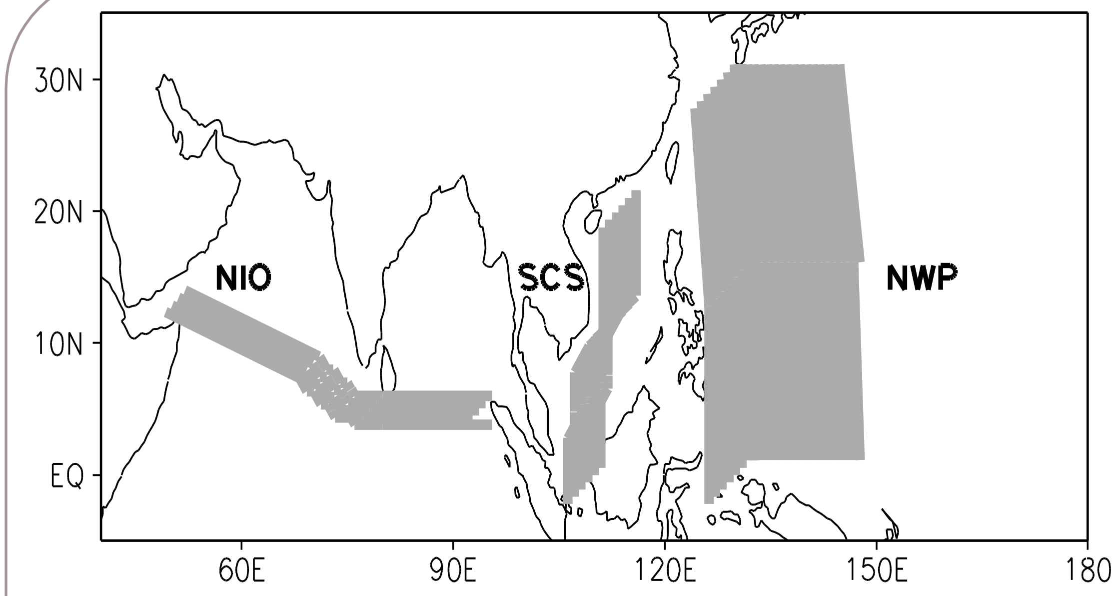

Data used

- Weather observations are essential for global and regional climate studies and prediction. We average the frequently traveled ship lanes data over three regions, the NIO, SCS and NW Pacific and this data along ship lanes are extracted from the International Comprehensive Ocean–Atmosphere Data Set (iCOADS) 2.5 (Woodruff et al. 2011).

- Surface wind velocity, SST, cloudiness, specific humidity and SLP are acquired. The record length of ~140 years (1870-2007) allows the investigation of the Indo-western Pacific climate variability associated with ENSO in different multi-decadal epochs.

- Observed station (e.g., Seychelles) rainfall data for 19th century is obtained from NOAA

- We make use of the gridded dataset of land monthly precipitation for the 1850-1995 of Dai et al. (1997) and the Center for Climate Prediction merged analysis for precipitation (CMAP; Xie and Arkin 1997) data.

- Philippine and Guam islands rain-gauge based precipitation data for the period of 1900 to 2007 are obtained from Monthly Bulletins of Philippine Weather Bureau (Kubota and Chan 2009).

- In addition to observational analysis, we use a 5 member ensemble mean of an AGCM the T85 TOGA (Tropical Ocean Global Atmosphere), forced by tropical (20°N-20°S) observed time-varying SSTs from January 1871 through September 2001 (http://www.cesm.ucar.edu). The model incorporates the climatological seasonal cycle of SSTs polewards of 30° latitude, with linear interpolation between 20° and 30°. The model simulations used are from the National Center for Atmospheric Research (NCAR) Community Atmospheric Model version 3 (CAM3) (Collins et al. 2006).

(Chowdary et al. 2012, J. Climate)

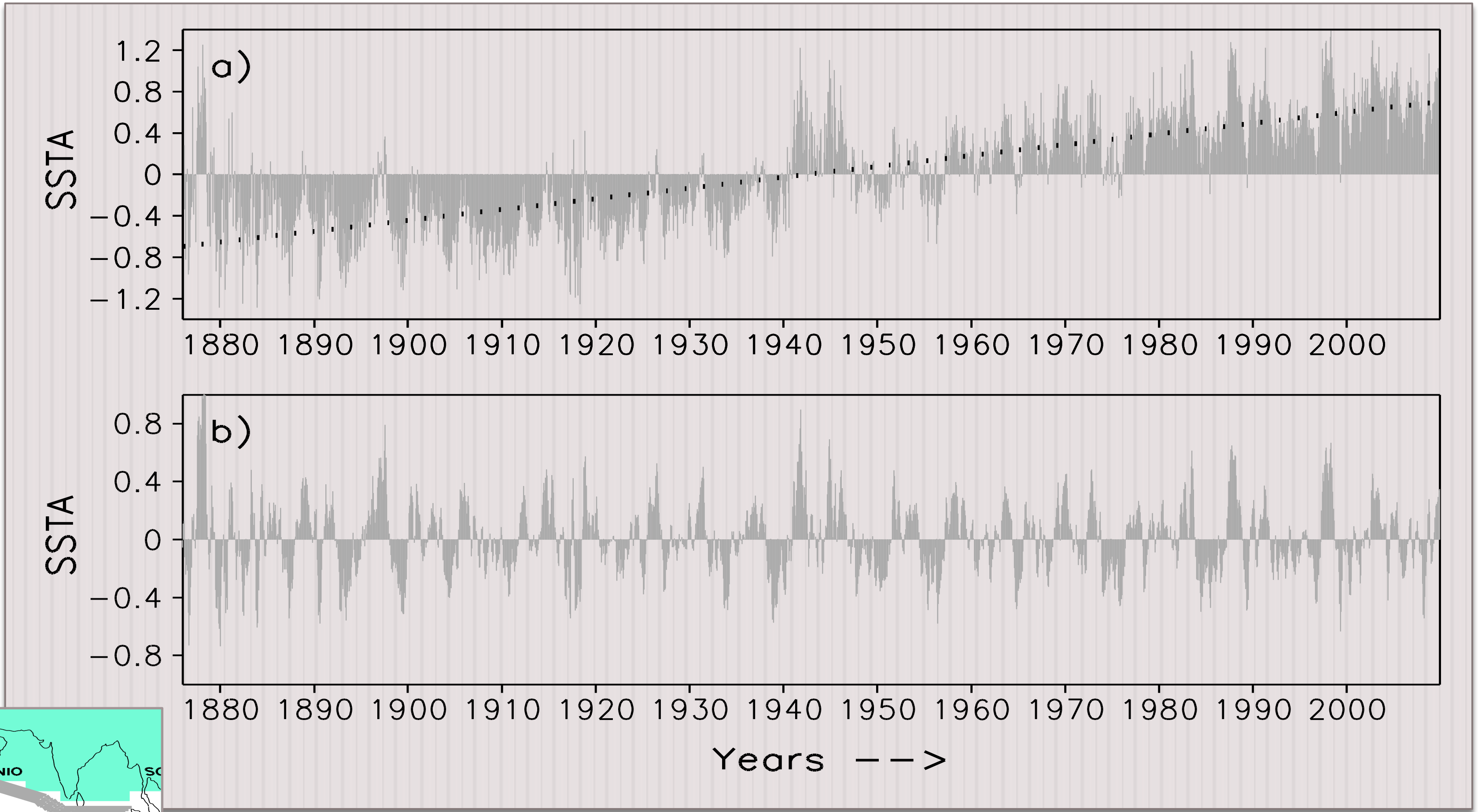

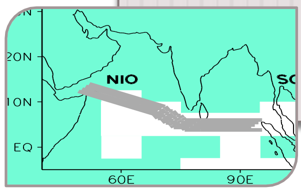

➢ **(a) Time series of monthly mean SST anomaly (°C) averaged along the NIO ship track for 1870-2007 and (b) time series after removing trend. Dotted line denotes the linear trend in (a).**

(Chowdary et al. 2012)

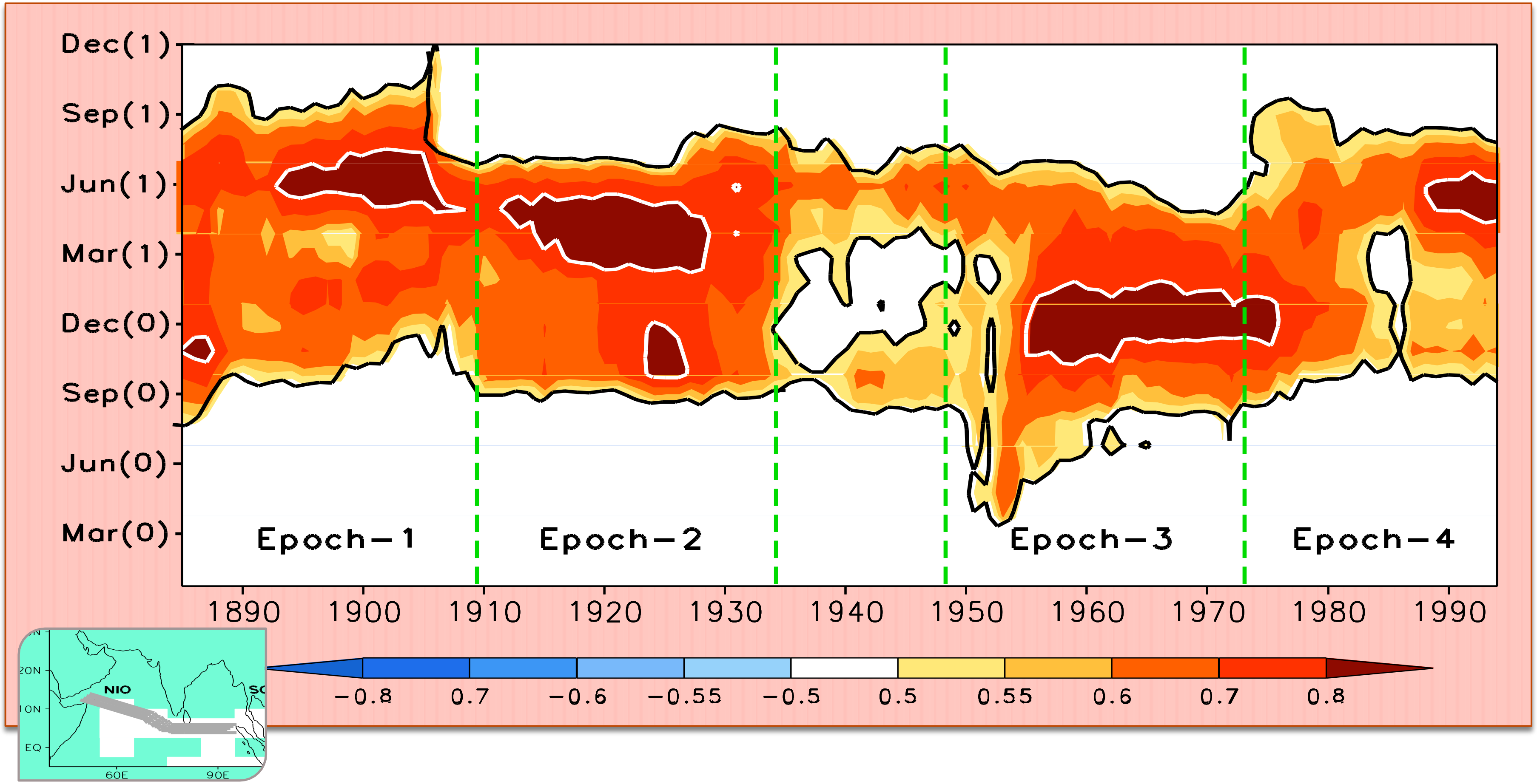

➢ Correlation (shaded) in 21-year sliding windows between NIO SST anomalies (averaged along ship track) and NDJ(0/1) Niño 3.4 index. Green dashed lines divide the data into four epochs to study the inter-decadal variations associated with ENSO. Solid and black contours represent the 95% confident level and white contours represent correlations above 0.8.

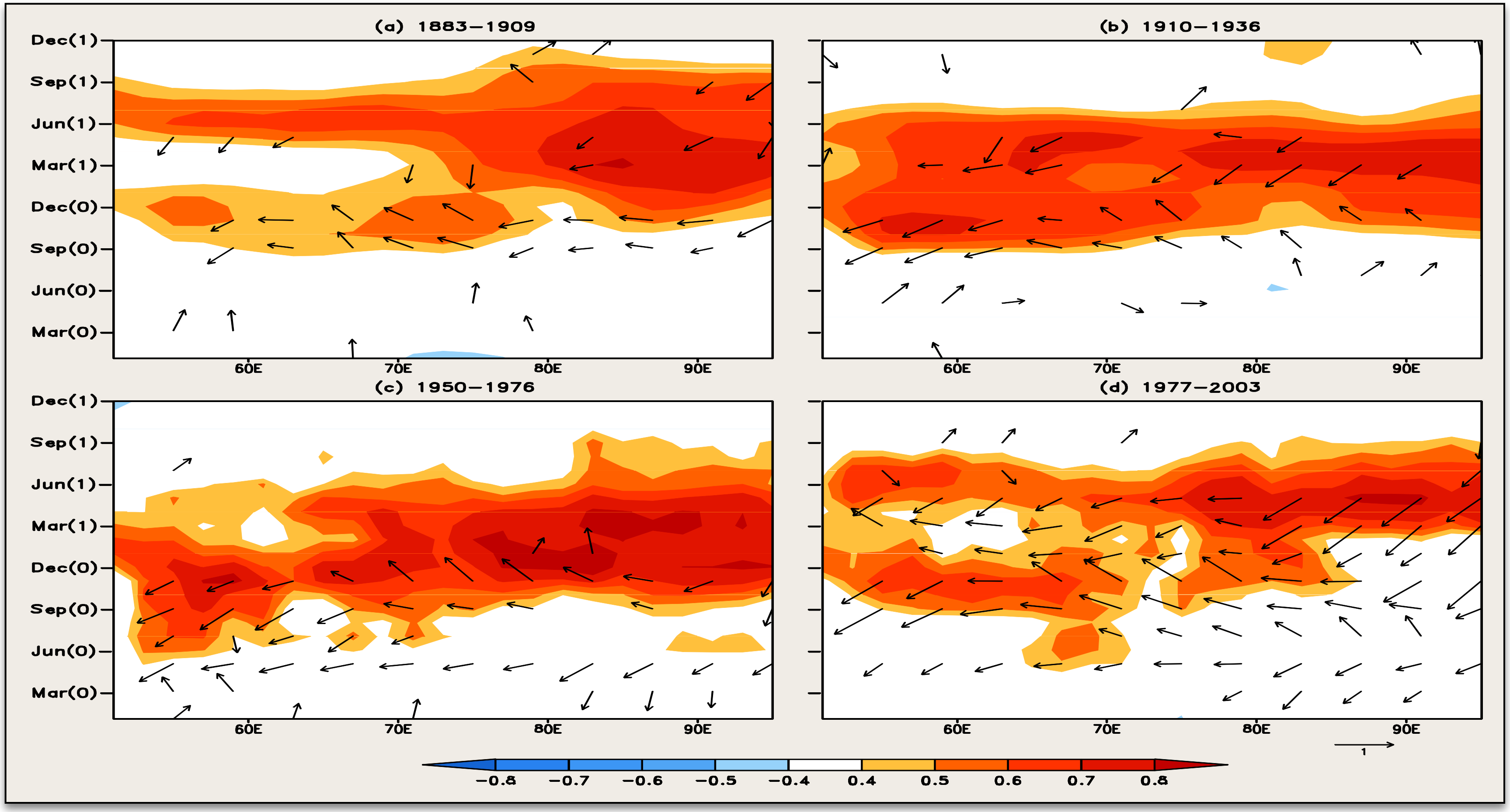

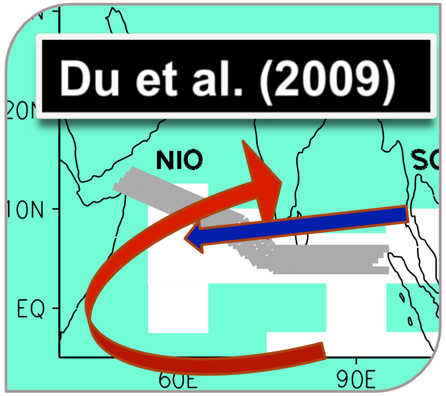

▪ Correlation of SST (shaded) and surface winds (vectors) along the NIO ship track, with the NDJ(0/1) Niño 3.4 index as a function of calendar month and longitude in (a) epoch-1 [1883-1909], (b) epoch-2 [1910-1936], (c) epoch-3 [1950-1976] and (d) epoch-4 [1977-2003].

From Du et al. 2009

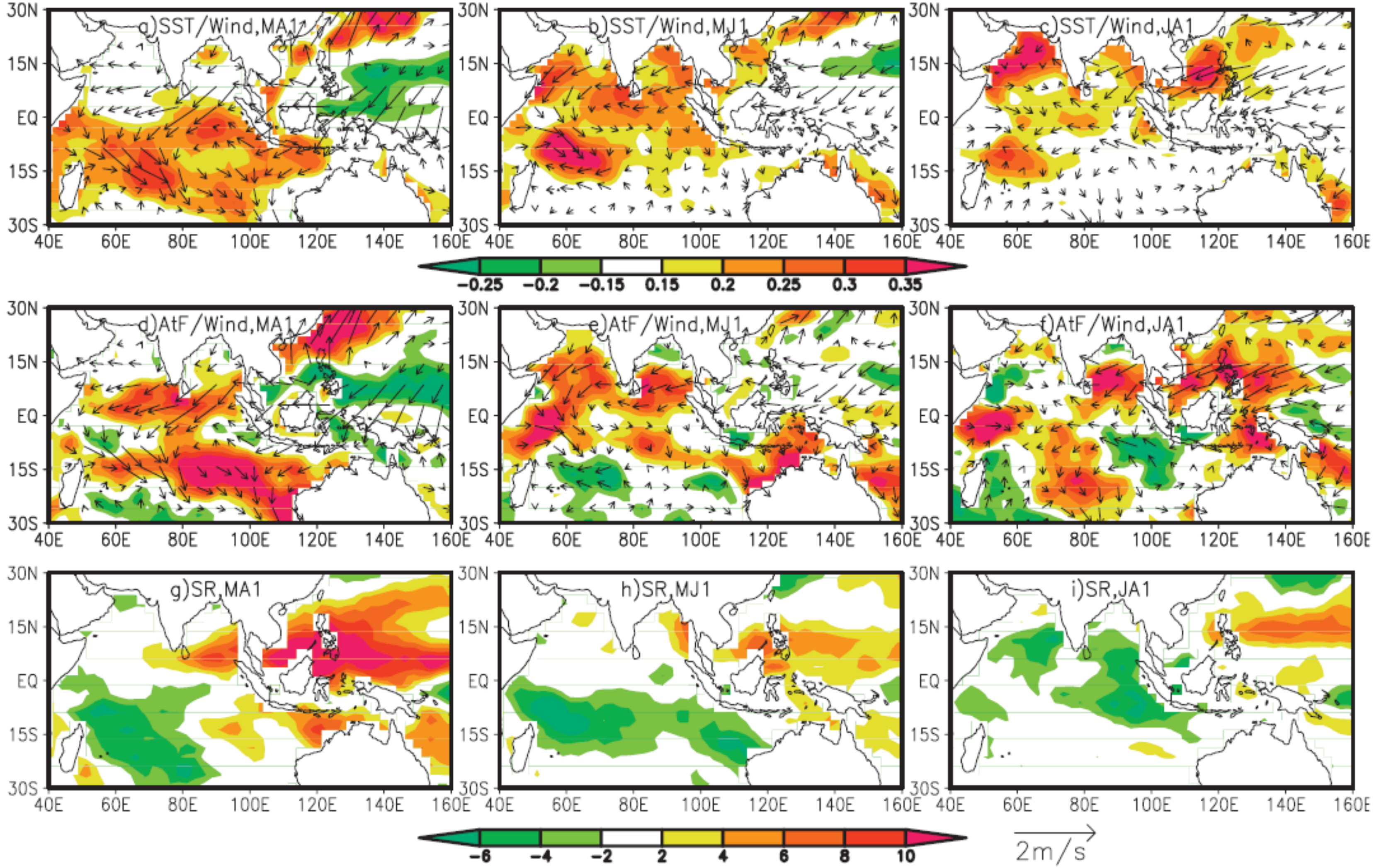

FIG. 8. SST (°C), wind velocity (m s^{-1}), and heat flux (W m^{-2}) anomalies expressed in regression upon the NDJ(0) Niño-3.4 index during (left) March–April(1), (middle) May–June(1), and (right) July–August(1). AtF stands for the atmospheric forcing component of latent heat flux, SR is the solar radiation from ISCCP.

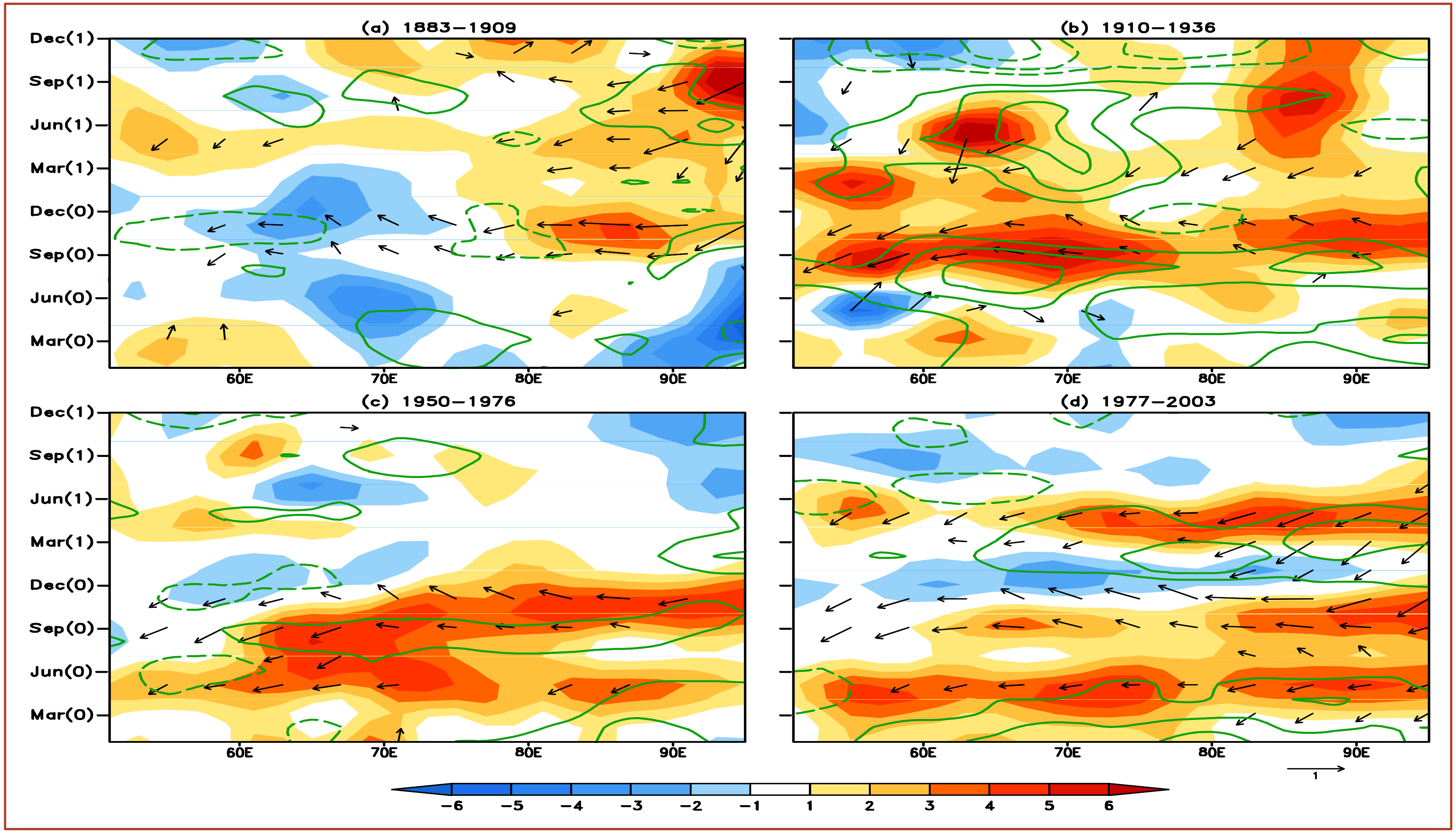

➢ Regression coefficients of AtF-L (shaded and white contours indicate values above 3.0 Wm^{-2}), surface winds (vectors; ms^{-1}) and short-wave radiation (green contours; Wm^{-2}) along the NIO ship track, upon the NDJ (0/1) Niño 3.4 index as a function of calendar month and longitude in (a) epoch-1, (b) epoch-2, (c) epoch-3 and (d) epoch-4. The contour (black) levels for short-wave radiation are ±1, ±2, ±3, and ±4 Wm^{-2}.

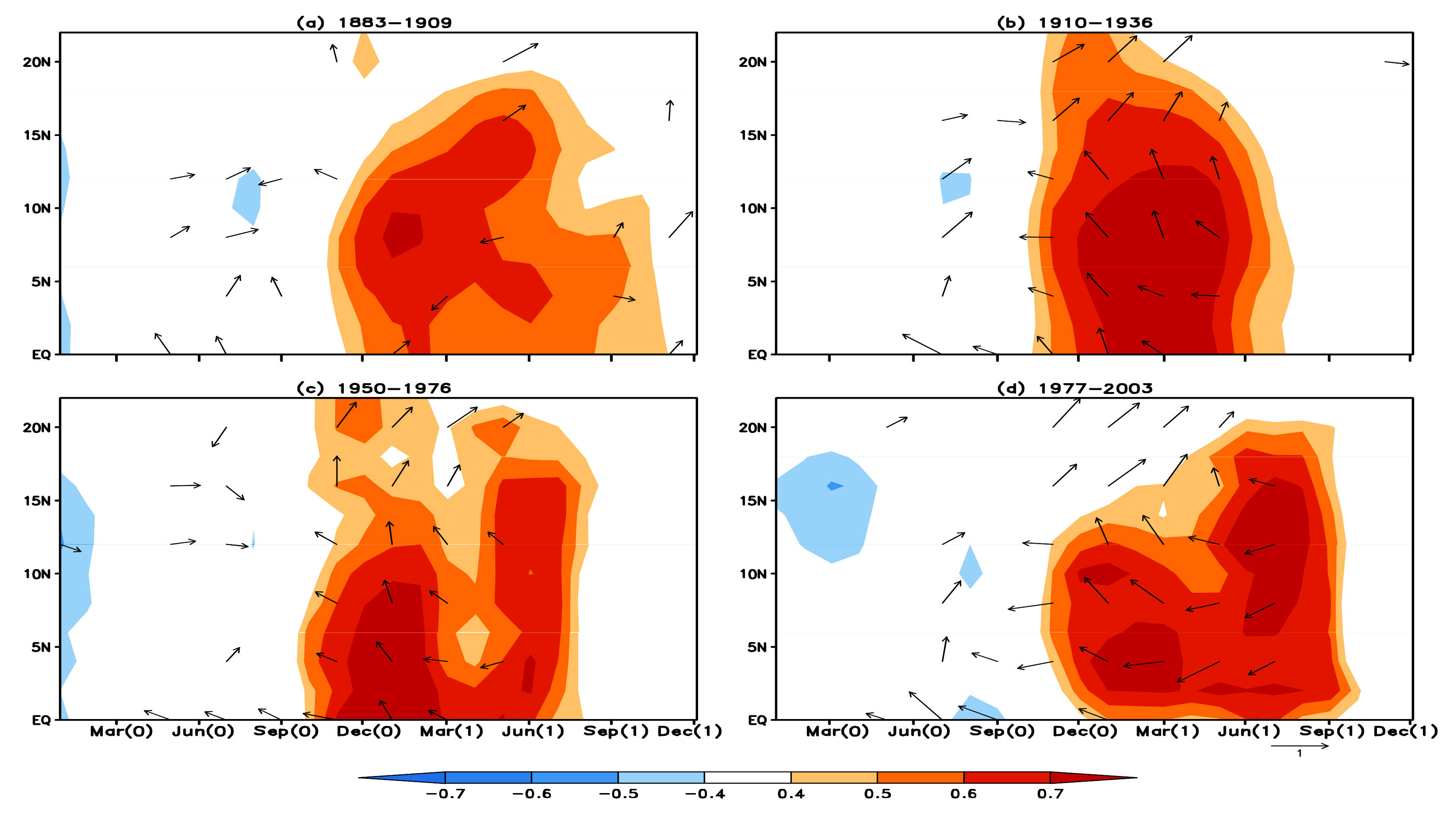

➢ **Correlation of SST (shaded) and surface winds (vectors) along the South China Sea ship track, with the NDJ(0/1) Niño 3.4 index as a function of calendar month and latitude for (a) epoch-1, (b) epoch-2, (c) epoch-3 and (d) epoch-4. Only values exceeding the 90% significance level are displayed (both for shading and vectors). Counters indicate a correlation magnitude above 0.6.**

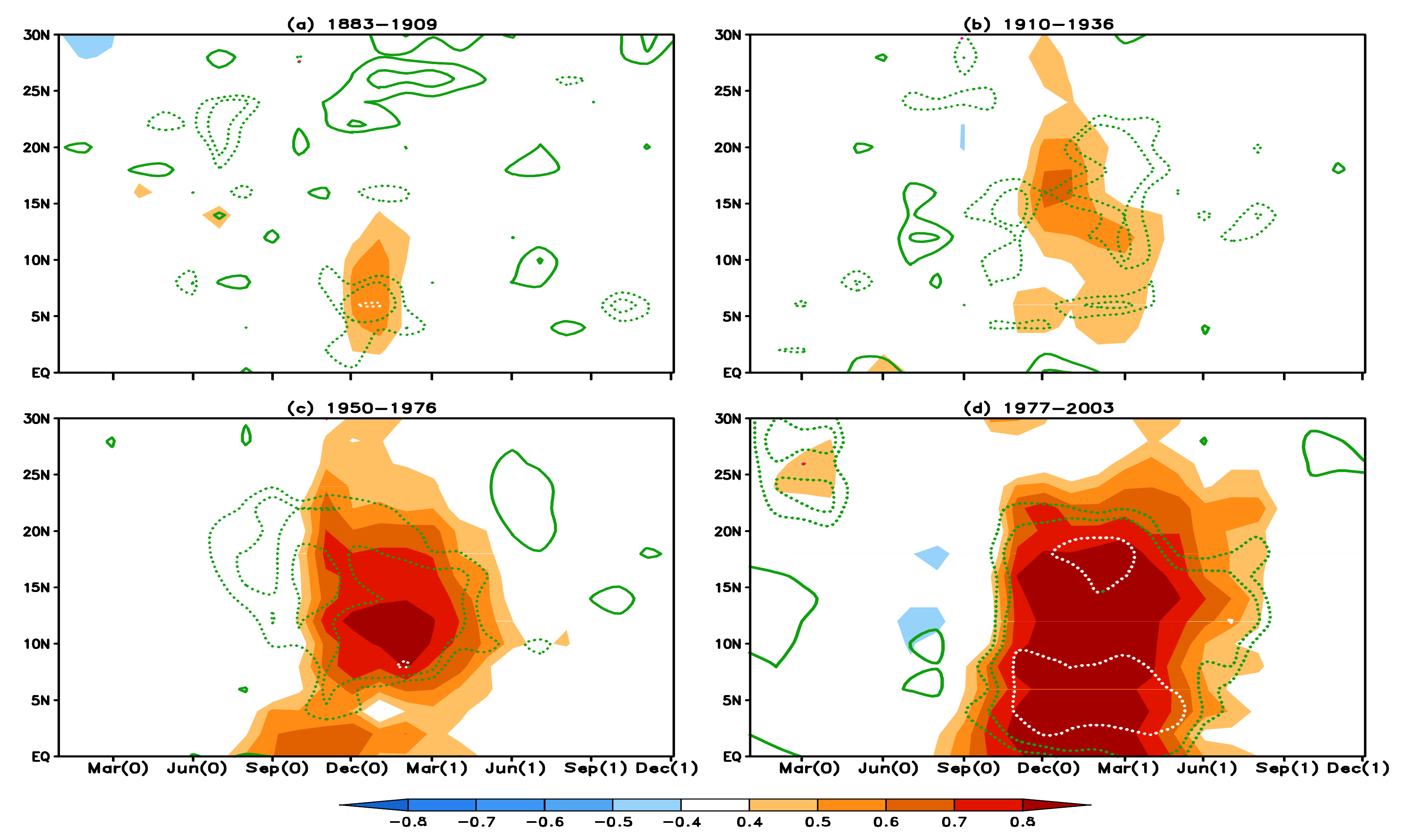

Correlation of SLP (shaded) and cloudiness (black contours) along the Northwest Pacific ship track (east of the Philippines) with the NDJ(0/1) Niño 3.4 index as a function of calendar month and latitude for (a) epoch-1, (b) epoch-2, (c) epoch-3 and (d) epoch-4. Contours for cloudiness correlations are shown at values of ±0.4, ±0.5, ±0.6, and ±0.7, with solid (dashed) contours indicating positive (negative) correlations.

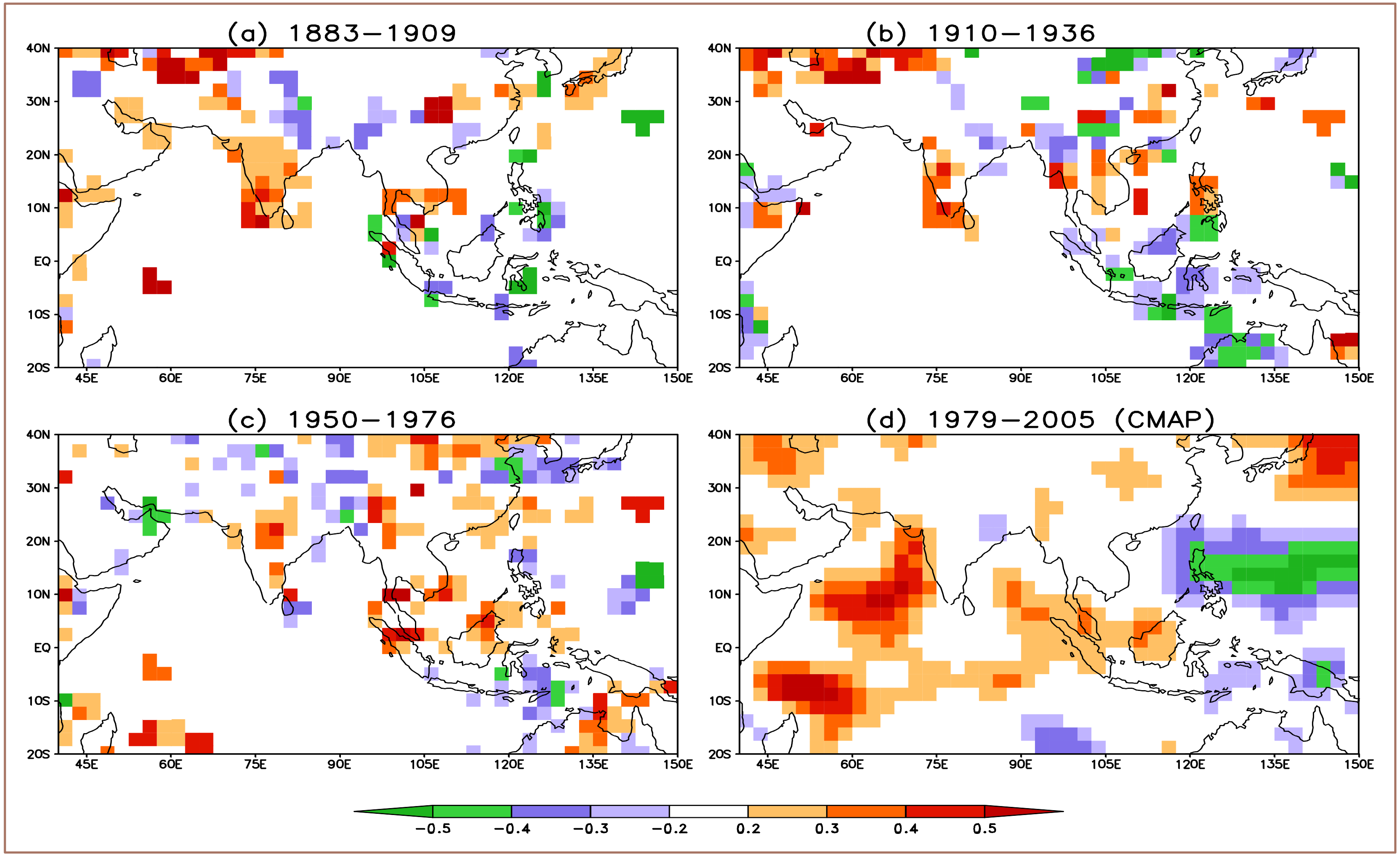

➢ JJA(1) correlation of land precipitation with the NDJ(0/1) Niño 3.4 index in (a) epoch-1, (b) epoch-2, (c) epoch-3, and (d) epoch-4. Land precipitation data are from Dai et al. (1997) for first three epochs and in epoch-4 precipitation data are obtained from CMAP.

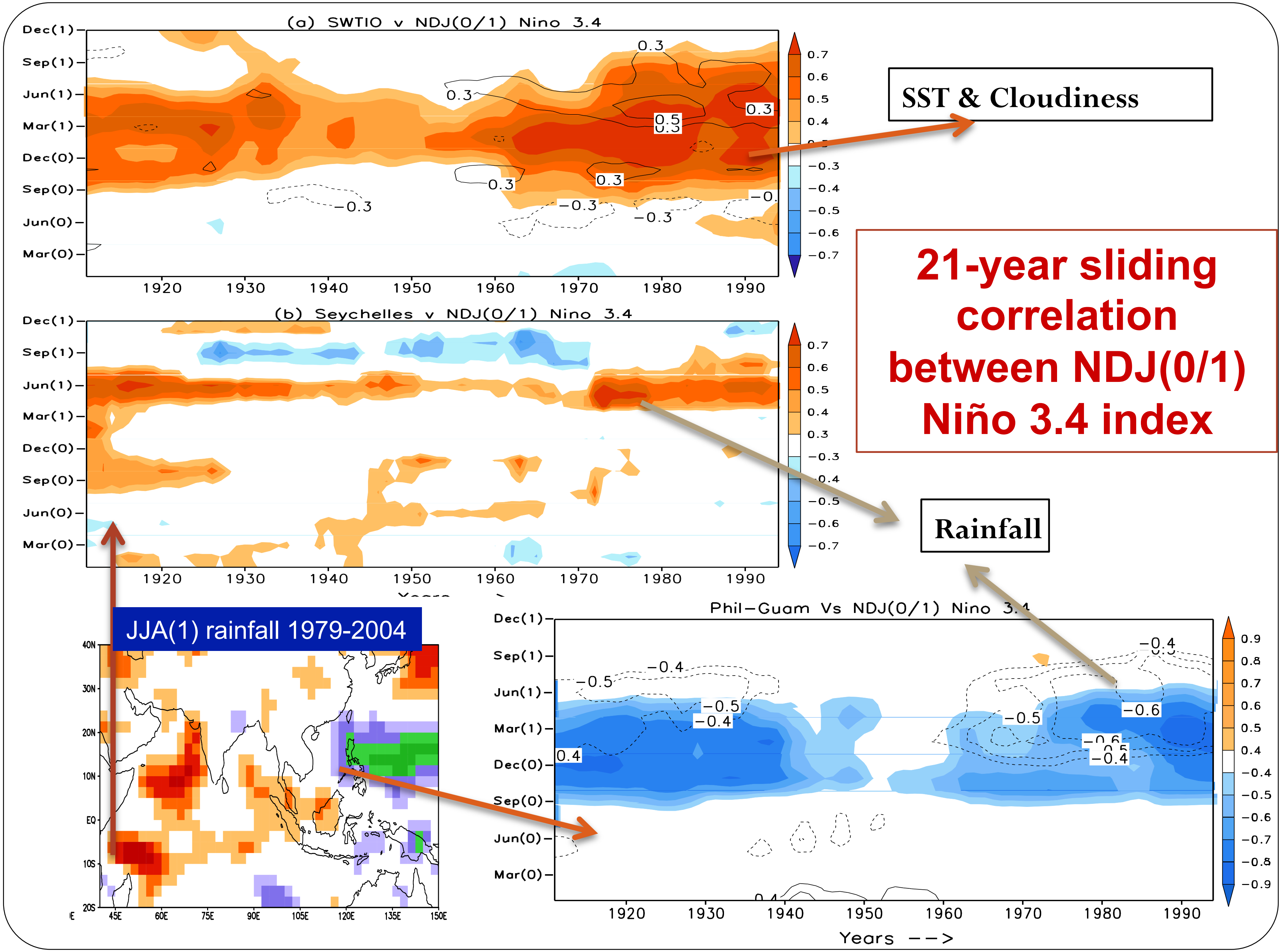

(a) SWTIO v NDJ(0/1) Nino 3.4
(b) Seychelles v NDJ(0/1) Nino 3.4
SST & Cloudiness
21-year sliding correlation between NDJ(0/1) Niño 3.4 index
Rainfall
JJA(1) rainfall 1979-2004
Phil–Guam Vs NDJ(0/1) Nino 3.4
Years -->

Atmospheric Model Simulations

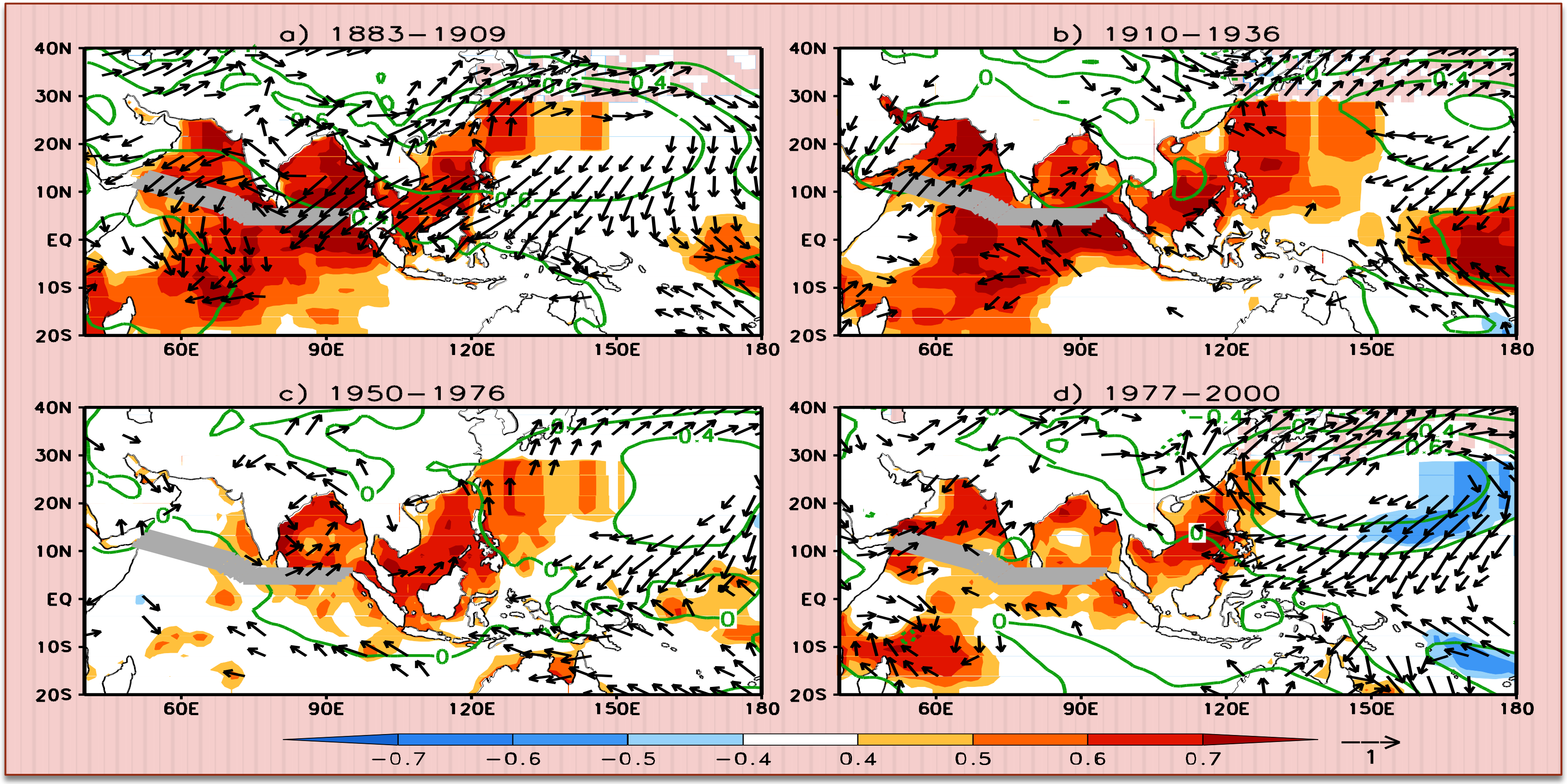

➢ **NDJ(0/1) Niño-3.4 SST index correlation with JJA(1) SST (shaded), SLP (contours) and surface wind velocity (vectors) from the ensemble mean of the CAM3 run for (a) epoch-1, (b) epoch-2, (c) epoch-3 and (d) epoch-4. NIO ship track is superimposed on model SST anomalies (thick black line).**

How does IO warming force NW Pacific anticyclone?

IO warming → Warm Kelvin wave into the WP
→ Northeasterly winds to the north under friction
→ Divergence over NW Pacific ←→ Suppressed convection

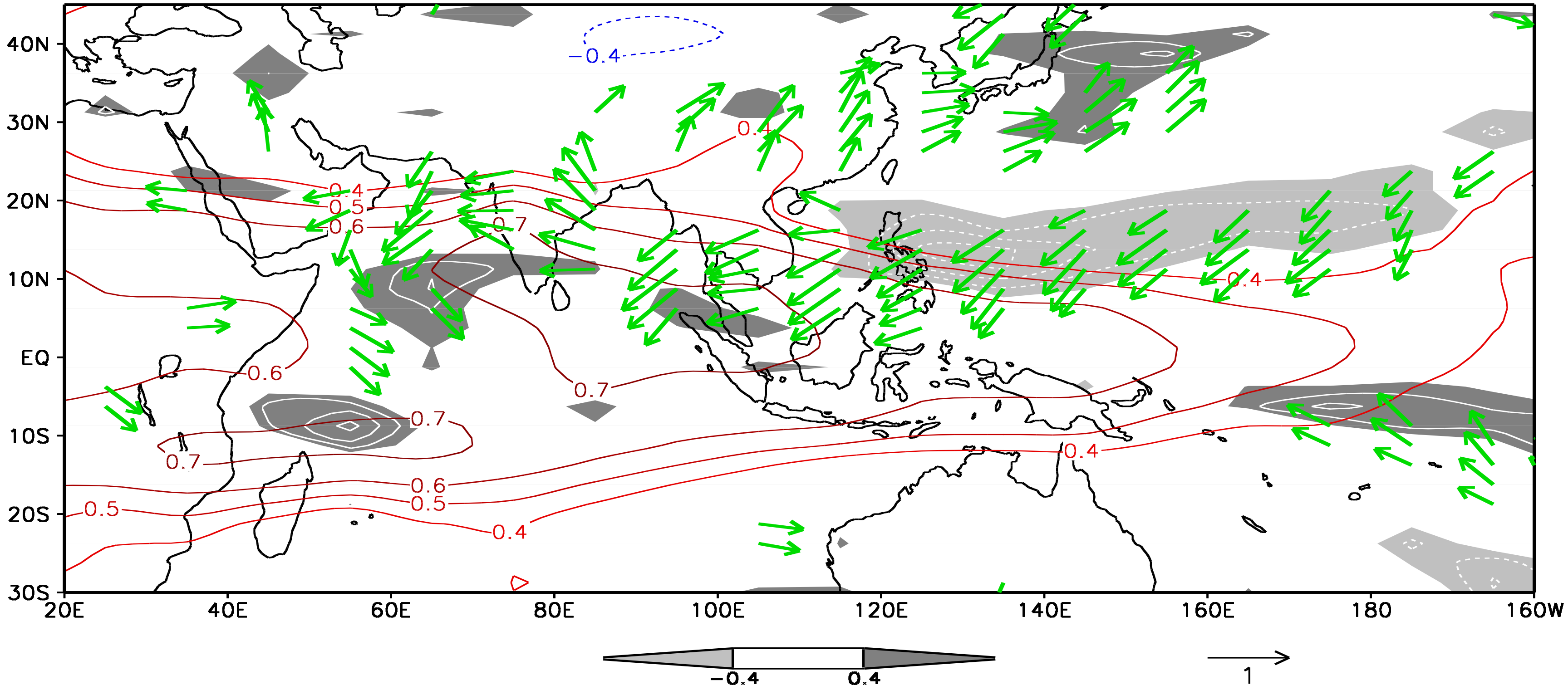

Tropospheric temp, surface wind & rainfall

Courtesy of S-P. Xie (IPRC), Xie et al. (2009).

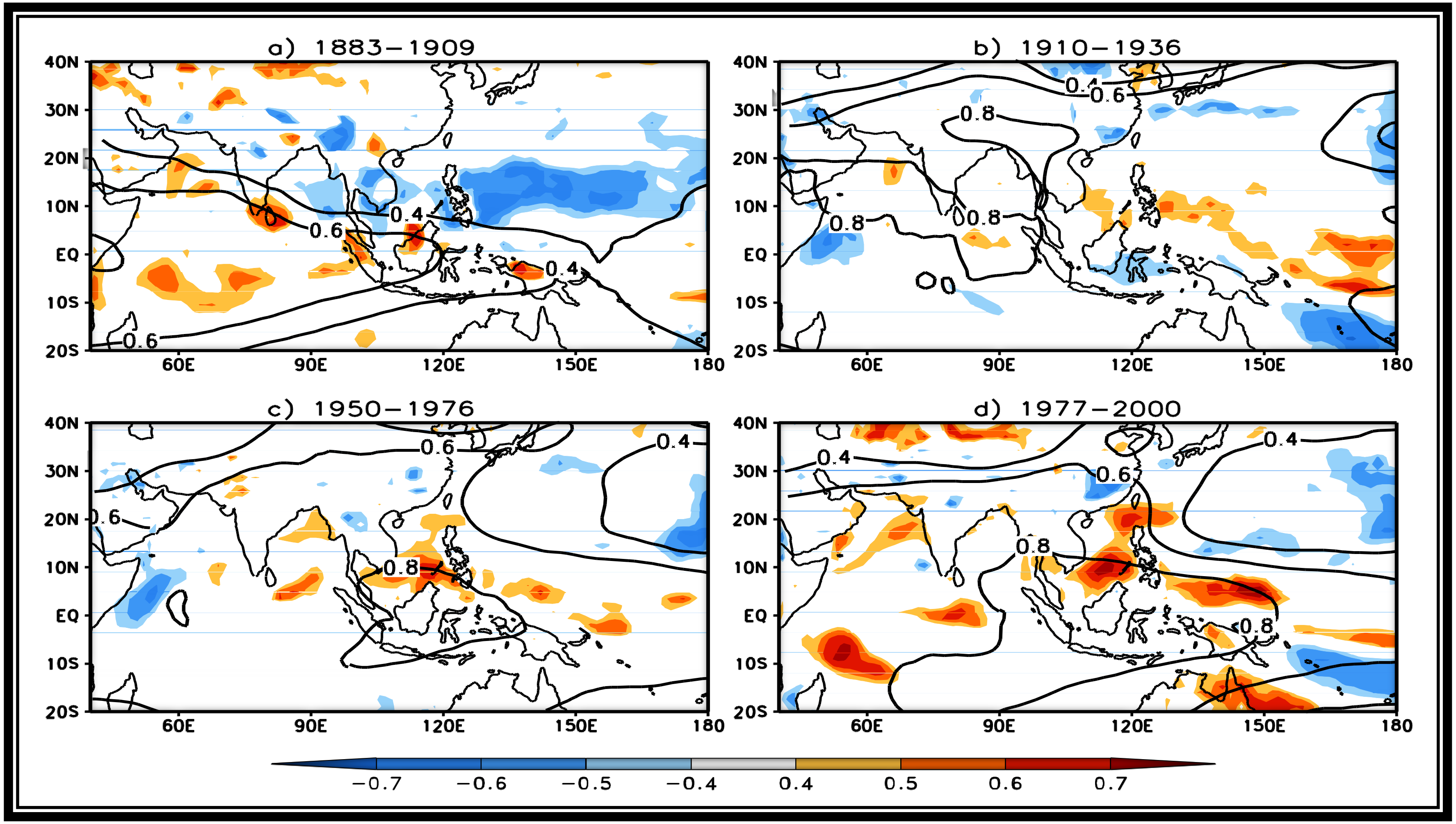

- NDJ(0/1) Niño-3.4 SST index correlation with JJA(1) **precipitation (shaded)** and **tropospheric temperature (contours)** from the CAM3 run for (a) epoch-1, (b) epoch-2, (c) epoch-3 and (d) epoch-4.

warm phase ***PDO*** *cool phase*

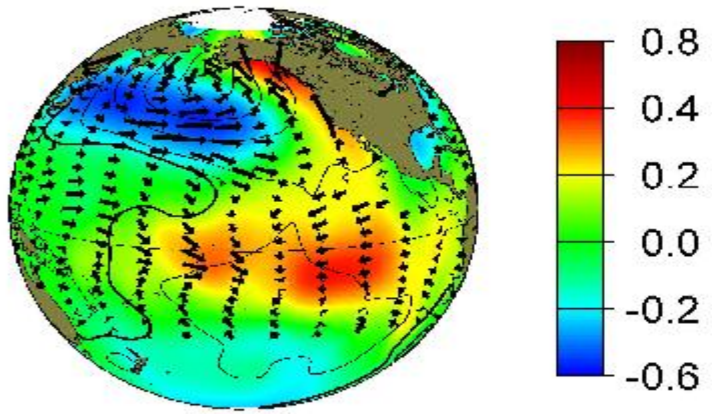

The "Pacific Decadal Oscillation" (PDO) is a long-lived El Niño-like pattern of Pacific climate variability. http://jisao.washington.edu/pdo/

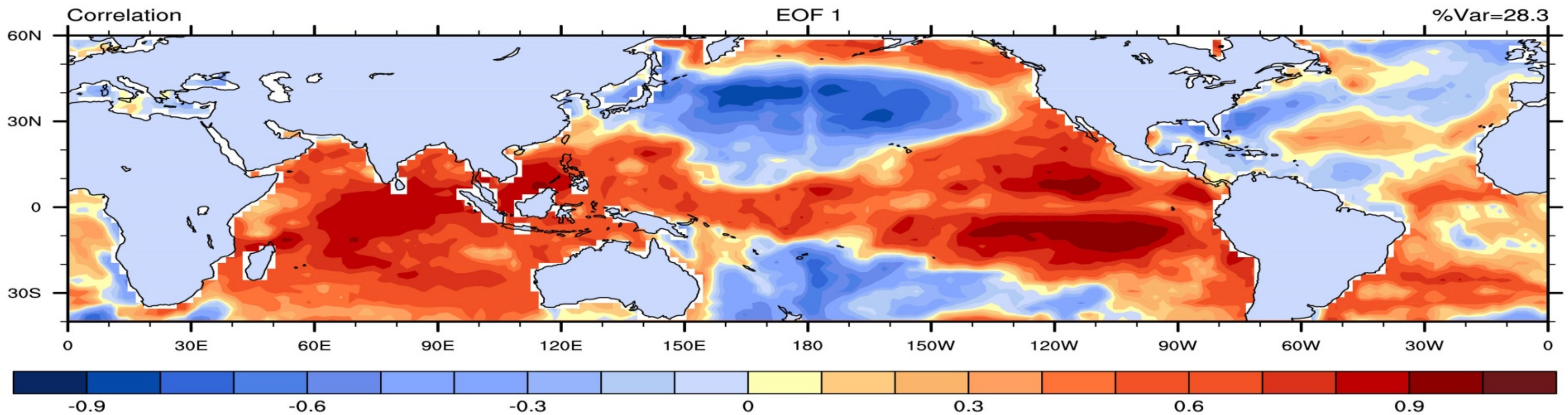

Pacific pattern strongly resembles the "Interdecadal Pacific Oscillation" (IPO, Power et al., 1999)

Chowdary et al. 2012 J. Clim.

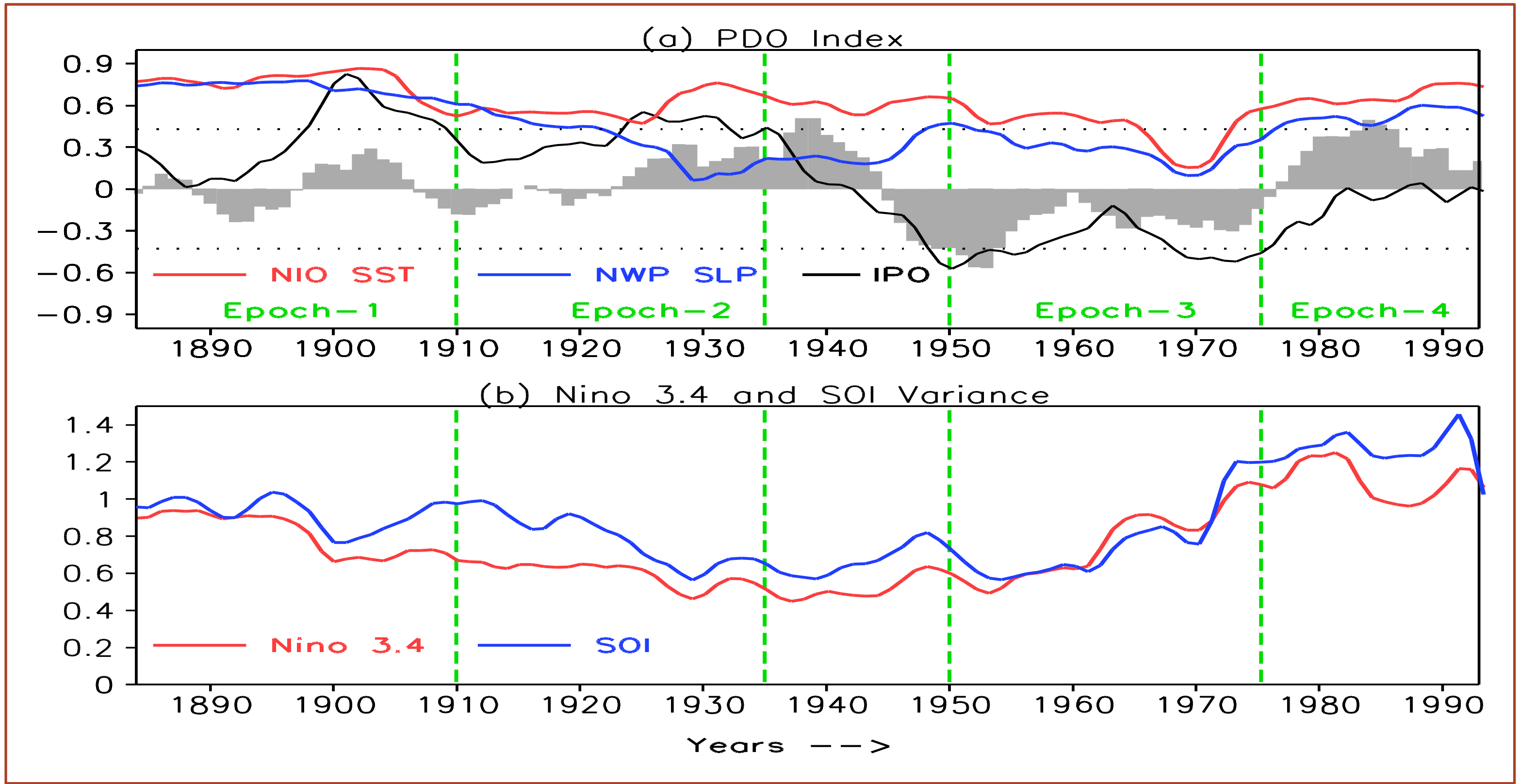

a) The time series of the PDO index (scaled by 2; gray bars), the IPO index (black line) and 21-year sliding correlations of NDJ(0/1) Niño-3.4 index with the JJA(1) NIO SST (averaged along ship track; red line) and Northwest Pacific SLP principal component (CAM3 run; blue line). (b) Time series of NDJ(0/1) Niño-3.4 index (red line) and DJF(0/1) SOI (scaled by 2.8; blue line) variance in 21-year sliding windows. Dotted lines denote the 95% significance level for sliding correlations in (a).

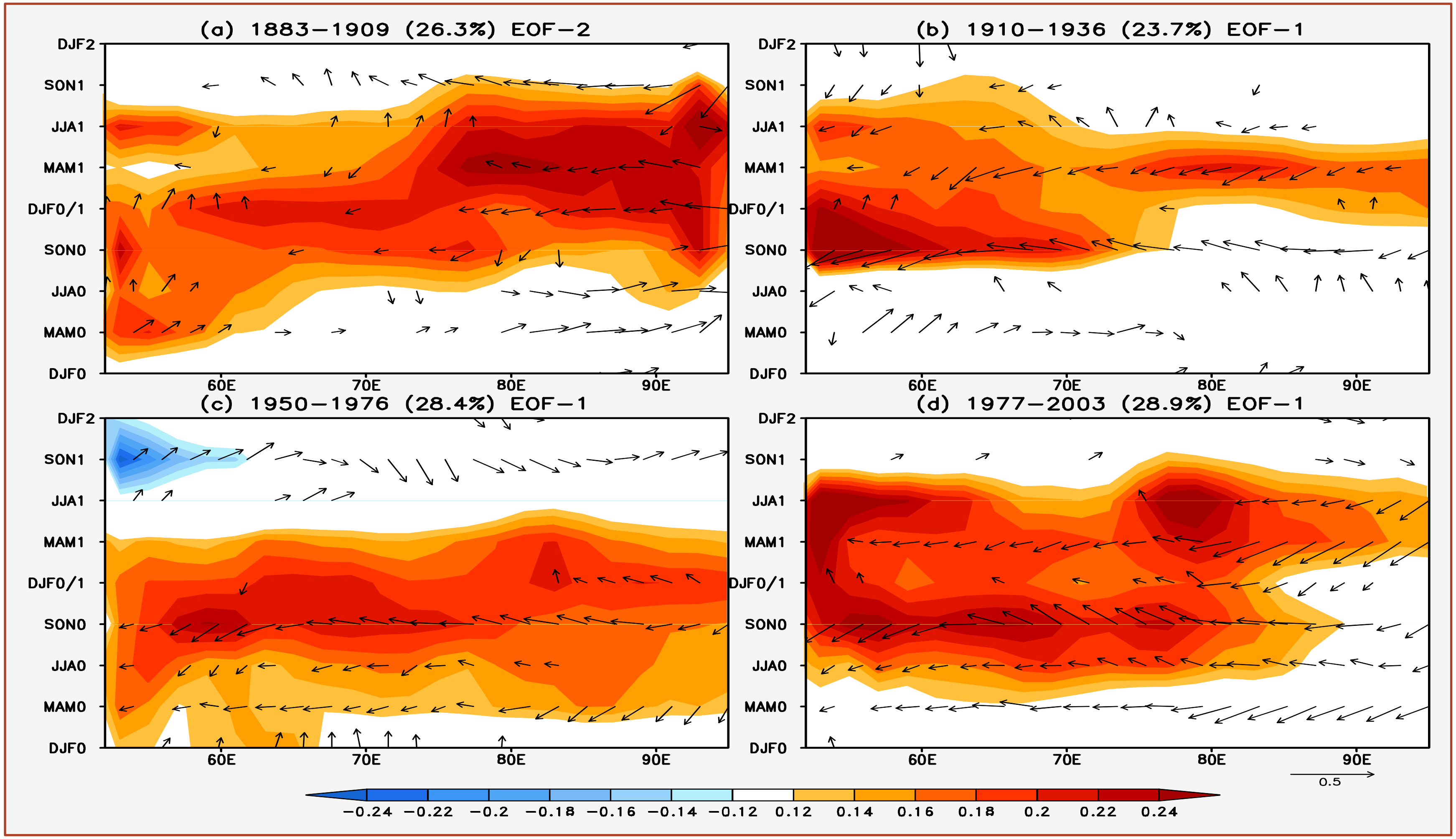

• ENSO-related S-EOFs of NIO ship track SST for the interval from DJF (0) [a year before the mature phase of El Niño] to DJF(2) [a year after the mature phase of El Niño] for (a) epoch-1, (b) epoch-2, (c) epoch-3 and (d) epoch-4.

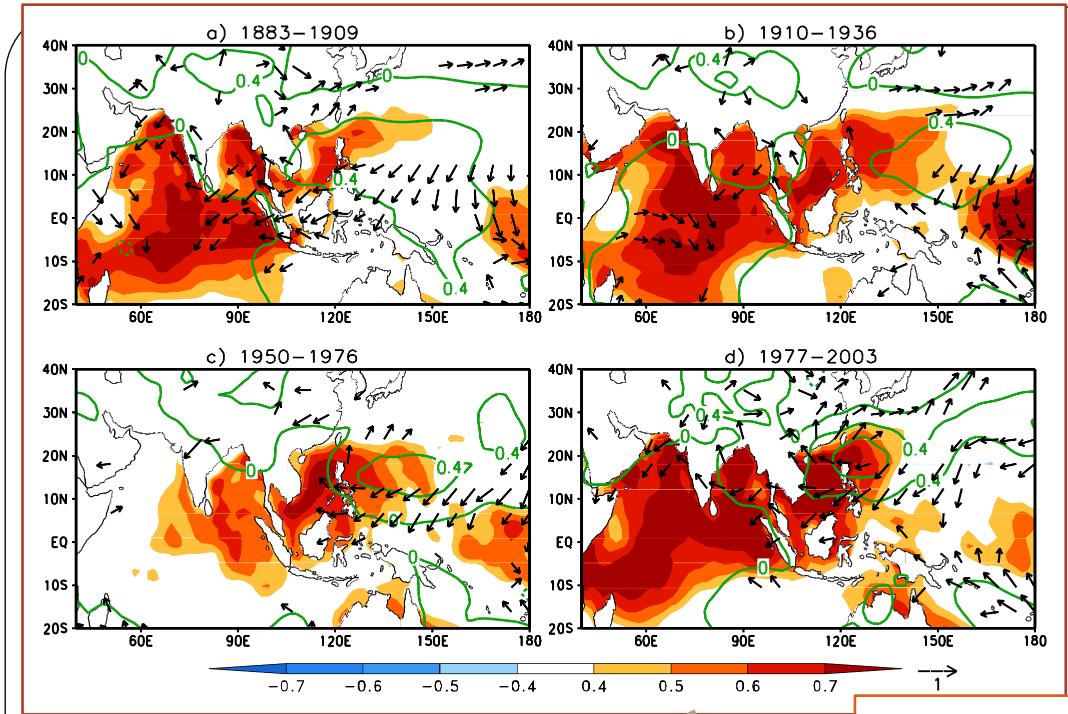

NDJ(0/1) Niño-3.4 SST index correlation with JJA(1) 2m temperature (shaded), SLP (black contours) and surface wind velocity (vectors) from 20CR.

SST
SLP
Surface wind

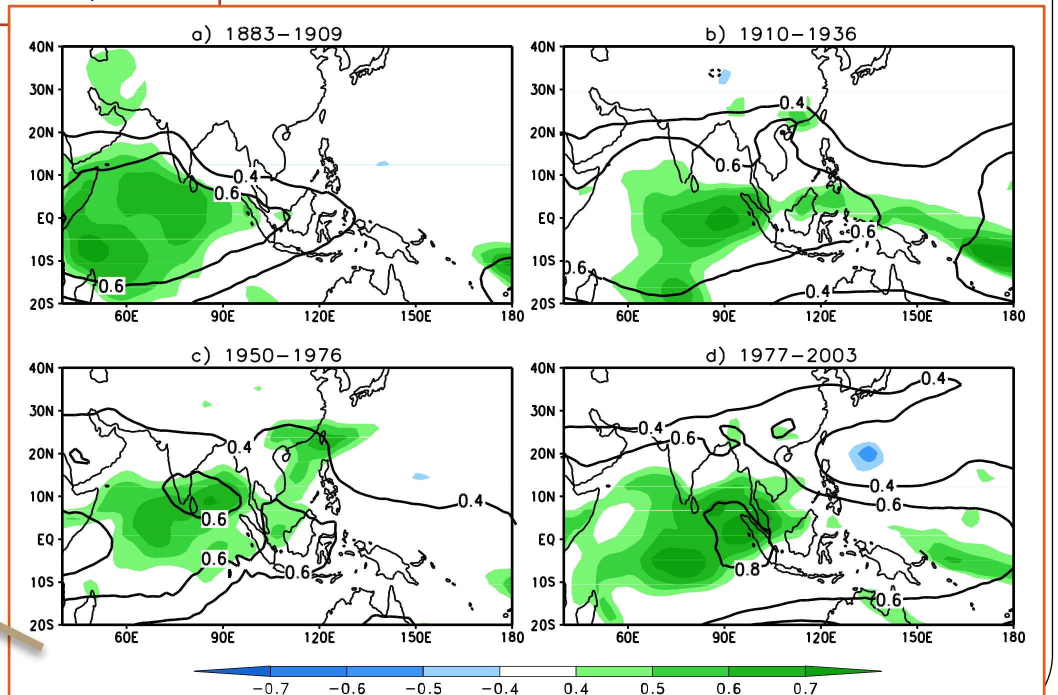

Precipitable water
Tropospheric Temperature

Summary

✓ The enhanced ENSO teleconnections occurred 100 years ago during the late 19th-early 20th century indicates that the recent strengthening of ENSO correlation over the Indo-western Pacific may not owe entirely to global warming but reflect natural variability.

✓ The above centennial modulation of ENSO teleconnection to the Indo- Northwest Pacific region is reproduced in an atmospheric general circulation model forced by observed SST.

✓ It is still interesting to ask how global warming affects ENSO teleconnection to the Indo-western Pacific (Zheng et al. 2011). Future studies need to investigate physical mechanisms for slow modulation of ENSO and its teleconnections.

Northwest Pacific Climate Predictability during summer and possible role of the Tropical Indian Ocean

J. S. Chowdary[1,2]

Shang-Ping Xie[2], Jing-Jia Luo[3,5], June-Yi Lee[2], Jan Hafner[2,] Swadhin Behera[3], Bin Wang[2] Yukio Masumoto[3,4], and Toshio Yamagata[3,4]

[1] Indian Institute of Tropical Meteorology, India
[2] International Pacific Research Center, University of Hawaii at Manoa, Honolulu, Hawaii
[3] Frontier Research Center for Global Change, JAMSTEC, Yokohama, Japan
[4] Department of Earth and Planetary Science, The University of Tokyo, Tokyo
[5]Centre for Australian Weather and Climate Research, Melbourne, Australia

Data:

- The hindcast data set is derived from 11 global coupled ocean-atmospheric general circulation models (CGCMs). They include seven coupled models from the European Center's Development of a European Multi-Model Ensemble System for Seasonal to Inter-Annual Prediction (DEMETER) database (Palmer et al. 2004) and four coupled models from the Asian-Pacific Economic Cooperation Climate Center (APCC)/Climate Prediction and its Application to Society (CliPAS) project [Wang et al., 2009].

- Model results are compared with: HadISST data [*Rayner et al*., 2003], NCEP reanalysis 2 [*Kanamitsu et al*., 2002] for SLP, geopotential height and winds at the 850 and 200 hPa levels and CMAP precipitation [*Xie and Arkin*, 1996].

- Various statistical methods are used such as empirical orthogonal function (EOF), correlation, regression and composites to evaluate model skills and to determine the physical mechanisms.

Details of Models: Analysis period is form 1980 to 2001 : MME is for 1982 to 2001

Abbreviation	Institute	AGCM	OGCM	Ensemble number and period	Reference
BMRC	BMRC-POAMA1.5	BAM 3.0d T47 L17	ACOM2 0.5–1.5°lat 2°lon L31	10; 1980–2002	Zhong et al. (2005)
CERF	CERFACS	ARPEGE T63L31	OPA 8.2 2° lat 2°lon L31	9;1980-2001	Palmer et al. (2004)
ECMW	ECMWF	IFS T95L40	HOPE-E 0.3-1.4° lat 1.4°lon L29	9;1980-2001	Palmer et al. (2004)
GFT1	GFDL	AM2.1 2°lat 2.5°lon L24	OM3.1 (MOM4) 1/3°lat 1°lon L50	10; 1979–2005	Delworth et al. (2006)
INGV	INGV	ECHAM4 T42L19	OPA8.1 0.5–1.5°lat 2°lon L31	9;1980-2001	Palmer et al. (2004)
LODY	LODYC	IFS T95L40	OPA8.2 2° lat 2°lon L31	9;1980-2001	Palmer et al. (2004)
METF	Météo-France	ARPEGE T63L31	OPA 8.0 182 GP × 152 GP L31	9;1980-2001	Palmer et al. (2004)
MAXP	MPI	ECHAM-5 T42L19	MPI-OM1 0.5–2.5°lat 2.5°lon L23	9;1980-2001	Palmer et al. (2004)
NCEP	NCEP	CFS T62 L64	MOM3 1/3°lat 1°lon L40	15; 1981–2004	Saha et al. (2006)
SINT	FRCGC- SINTEX-F	ECHAM4 T106 L19	OPA 8.2 2°cos(lat) 2°lon L31	9; 1982–2004	Luo et al. (2005)
UKMO	Met Office	HadAM3 2°lat 3.75°lon L19	GloSeaOGCM 0.3–1.25°lat 1.25°lon L40	9; 1980–2001	Palmer et al. (2004)

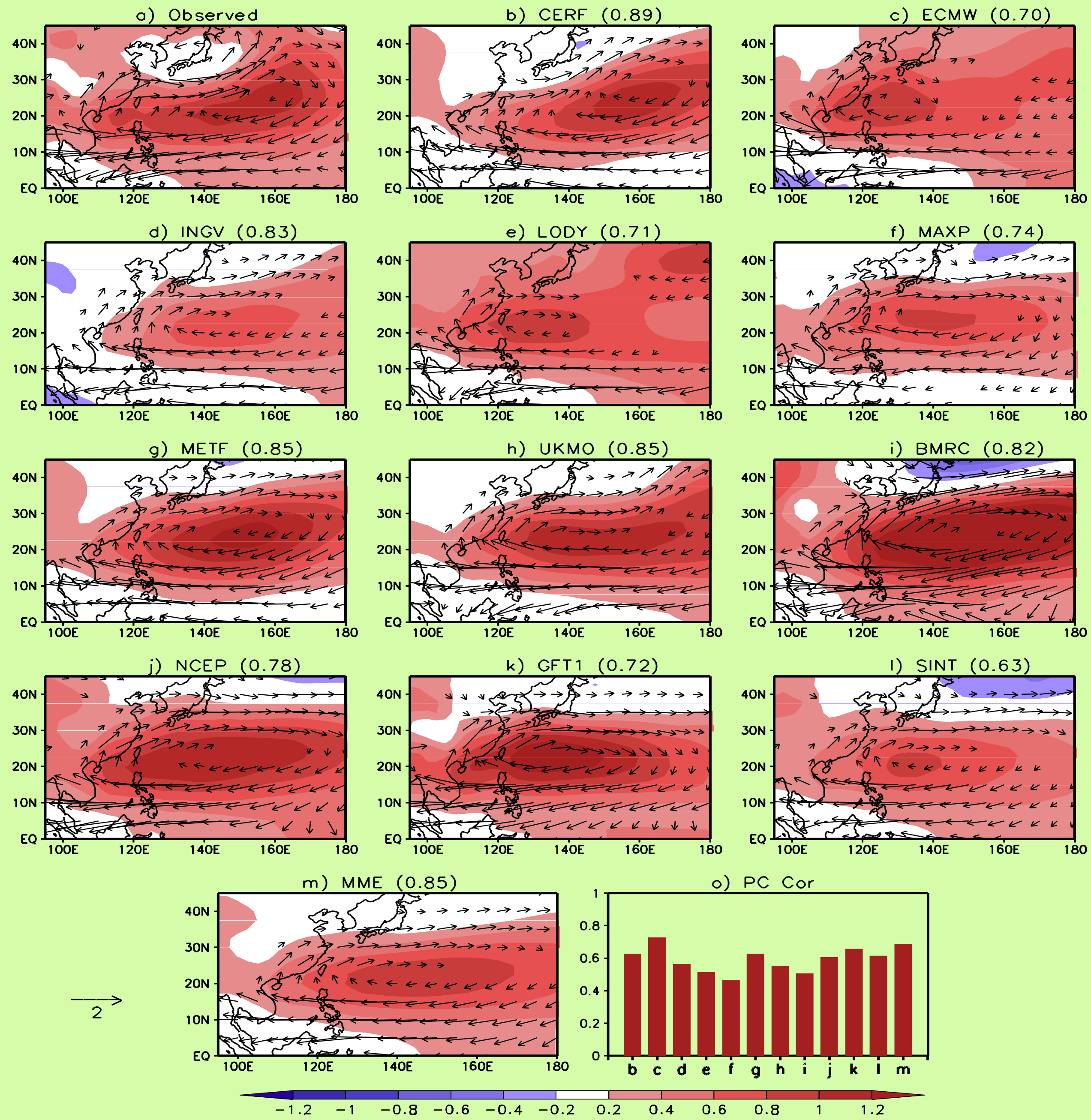
a) Observed
b) CERF (0.89)
c) ECMW (0.70)
d) INGV (0.83)
e) LODY (0.71)
f) MAXP (0.74)
g) METF (0.85)
h) UKMO (0.85)
i) BMRC (0.82)
j) NCEP (0.78)
k) GFT1 (0.72)
l) SINT (0.63)
m) MME (0.85)
o) PC Cor
40N
30N
20N
10N
EQ
100E
120E
140E
160E
180
2
b c d e f g h i j k l m
-1.2 -1 -0.8 -0.6 -0.4 -0.2 0.2 0.4 0.6 0.8 1 1.2

Rainfall EOF-2

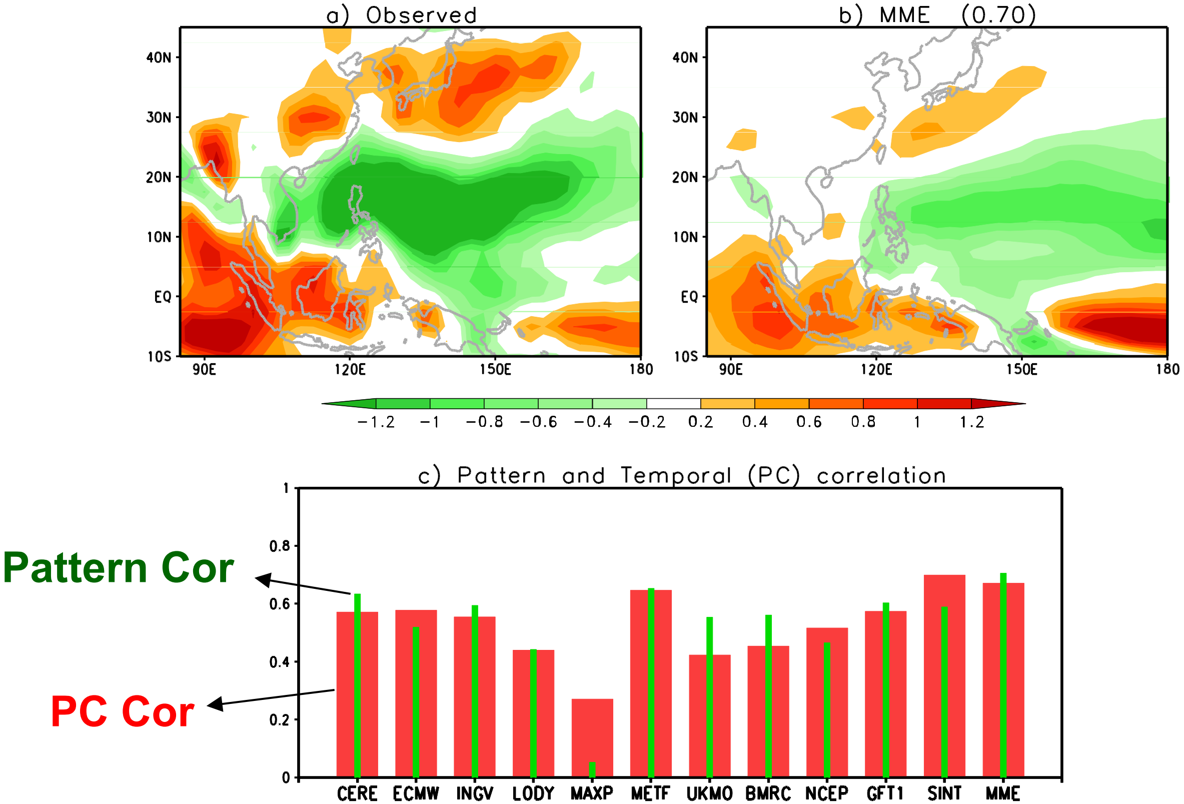

Chowdary et al. 2010 JGR Atmos.

The second EOF of JJA rainfall anomalies (hPa) obtained from (a) observations and (b) MME. (c) Pattern (green) Temporal (red) correlation in PC between observations and each model.

✓In comparison with observations, there is a southward displacement of positive rainfall anomalies over the Japan in most models.

✓Except MAXP, all models displayed reasonable skills in predicting the JJA (1) rainfall over the NW Pacific at one-month lead. Temporal correlation of PC also exceeds 0.43 in most models, significant at 95% confidence level.

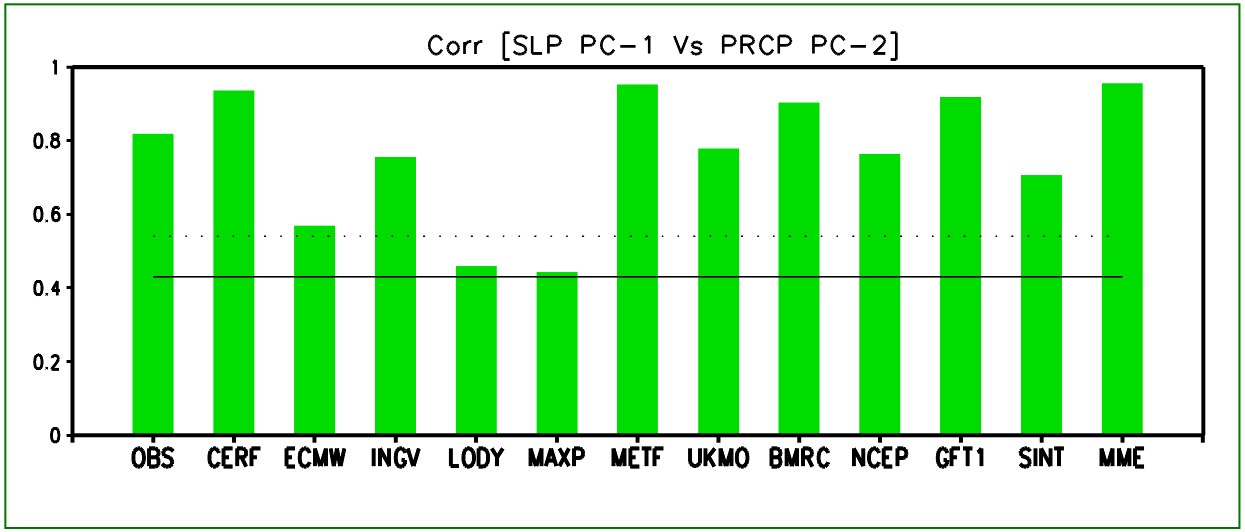

Correlation between the NW Pacific SLP PC-1 and precipitation PC-2 for observations, individual models and MME based on one-month lead prediction. Solid and dotted lines represent 95% and 99% confident levels, respectively.

✓Correlation coefficient between the first SLP PC and the second rainfall PC is 0.8 for observations and 0.95 for the MME prediction.

✓Some models (LODC, and MAXP) far underestimate the relationship. These models tend to have low skills for the second rainfall PC.

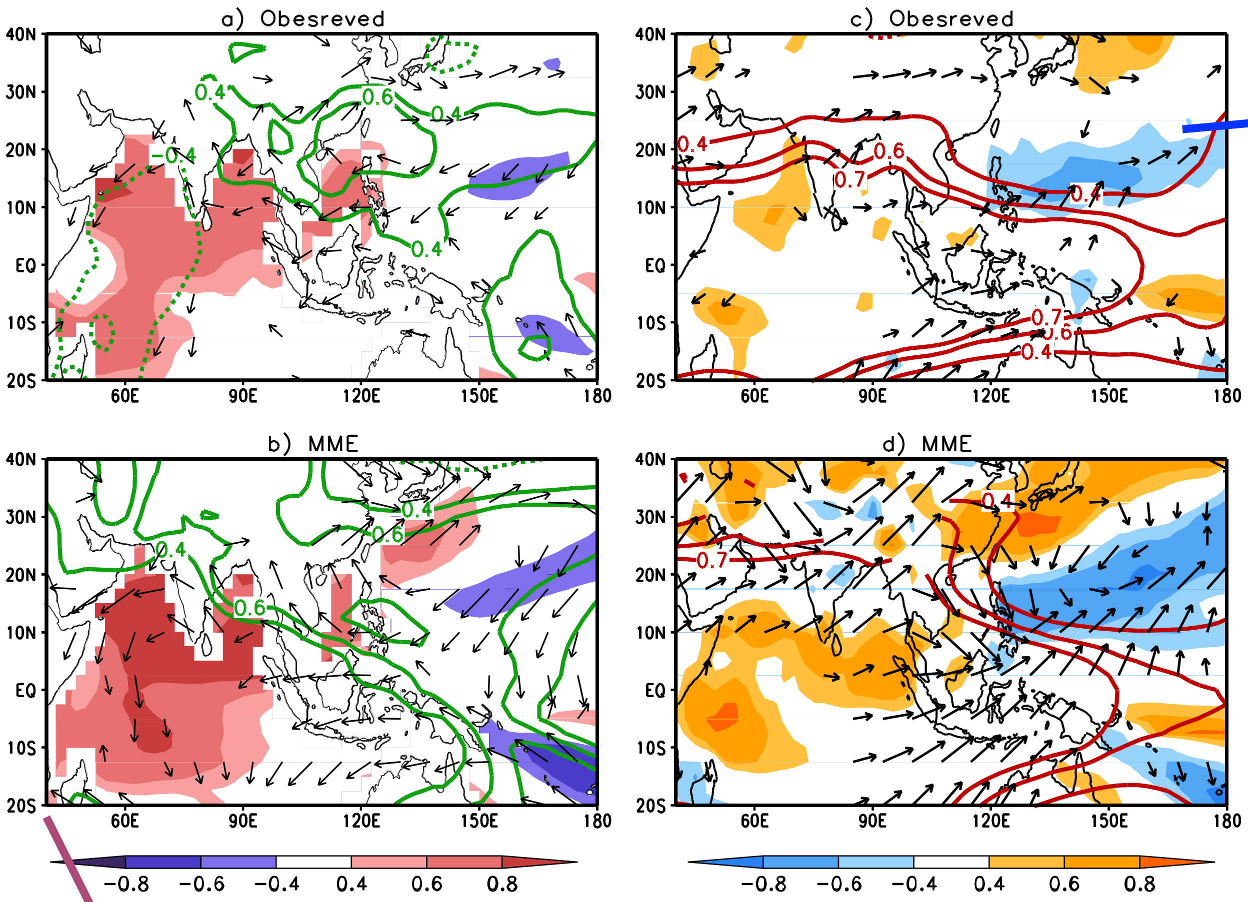

Rainfall (shaded)
TT (contour)
200hpa winds

NDJ(0) Niño-3.4 SST index correlation with JJA(1).

SST (shaded)
SLP (contour)
850hpa winds

Chowdary et al. 2010 JGR Atmos.

ENSO-Teleconnections are well represented in MME one-month lead prediction.

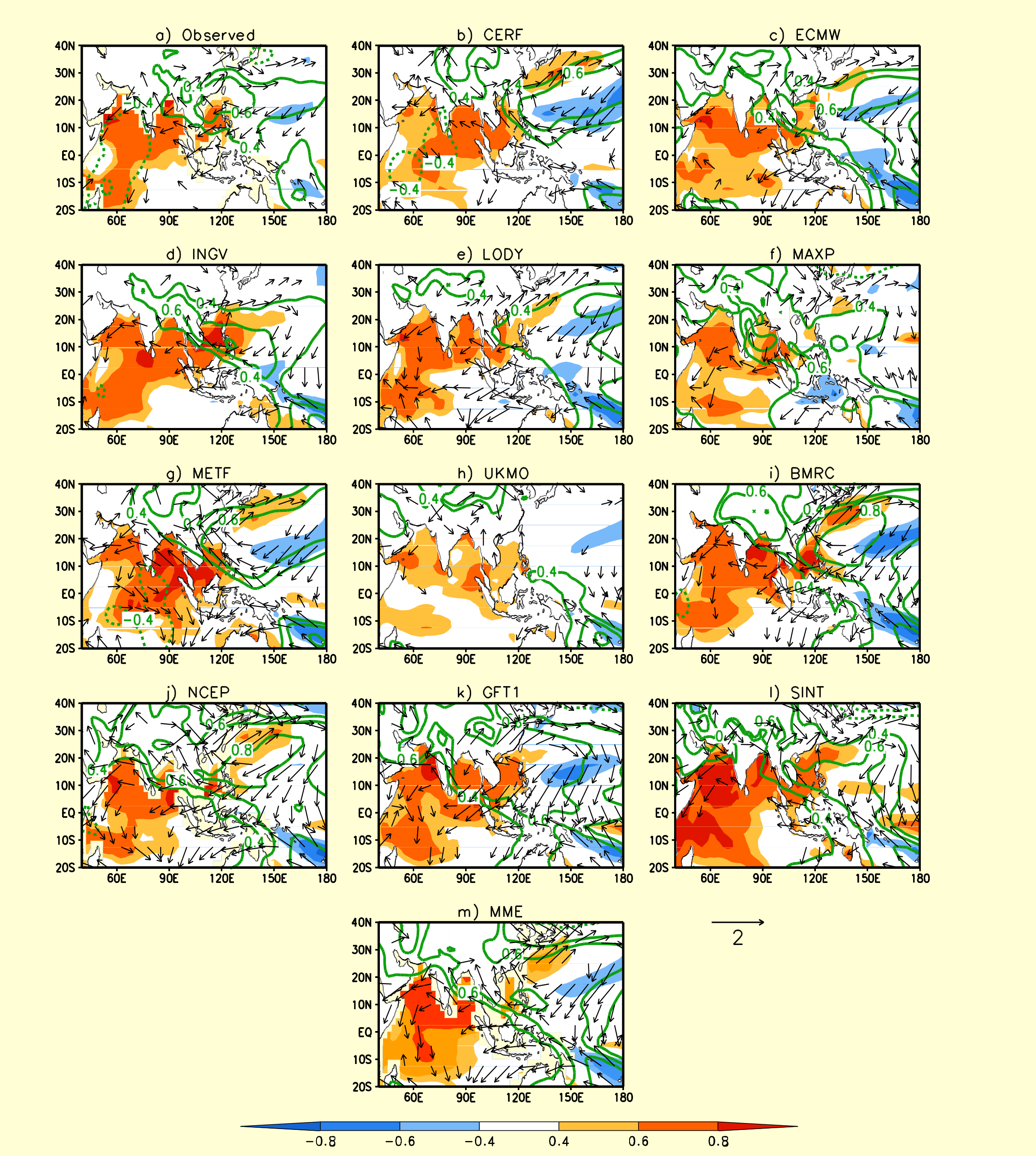

✓Most models capture positive SST correlations over the western and northern Indian Ocean (NIO), consistent with observations.

✓Many models reproduce the SLP correlation distribution over the NW Pacific in one-month lead prediction.

✓A few models failed to predict the weak negative SST anomaly over NW Pacific.

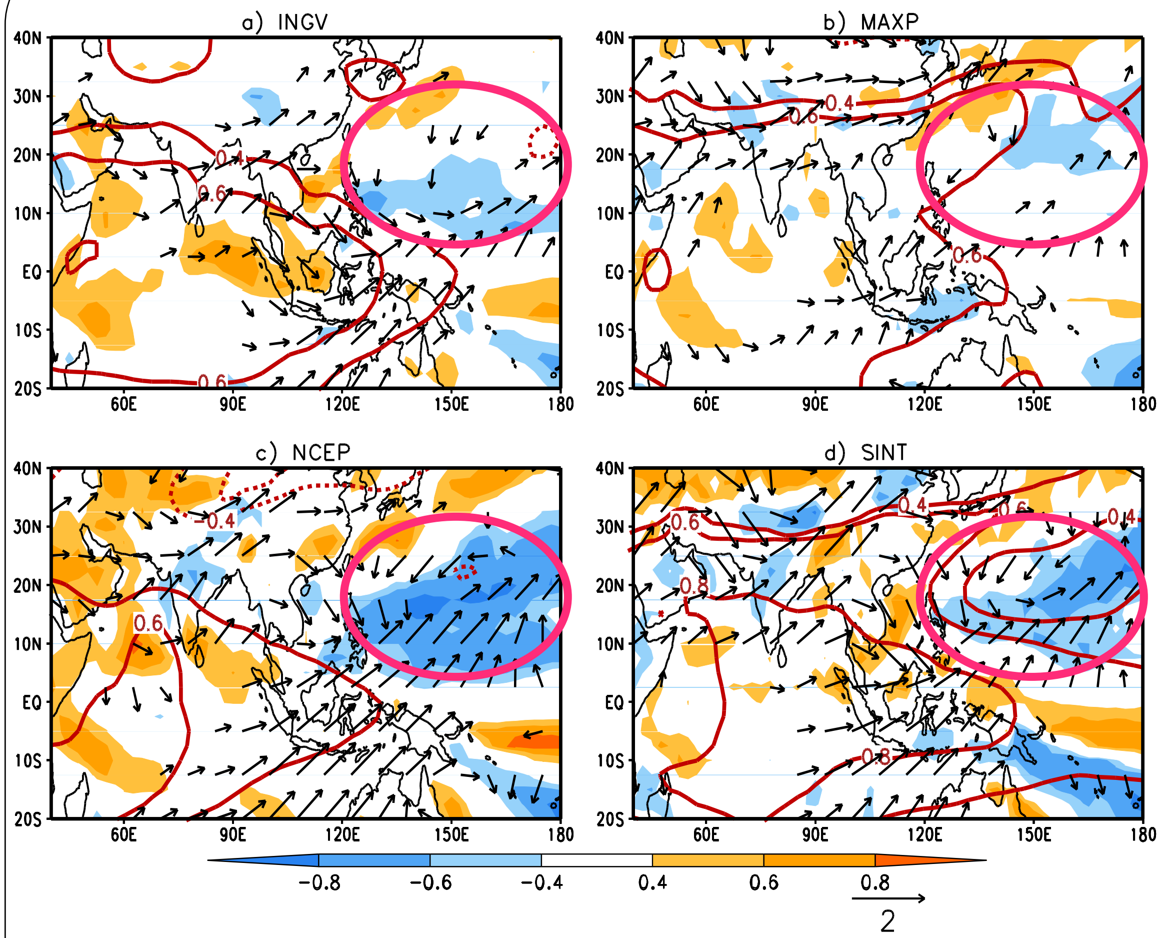

NDJ(0) Niño-3.4 SST index correlation with JJA(1) precipitation (shaded), tropospheric temperature (contours) and 200hPa wind velocity (vectors)

✓All models show the negative correlation of precipitation over the southeast flank of the 850 hPa anticyclonic anomalies in the NW Pacific in JJA(1).

✓Upper level (200hPa) winds and TT show significant variations over the Indo-western Pacific during JJA(1)

Composites of summer following El Niño

Chowdary et al. 2010 JGR Atmos.

Strengthened westerly jet and rainfall

SST (shaded; °C), SLP (contours; hPa) and 850hPa wind anomalies

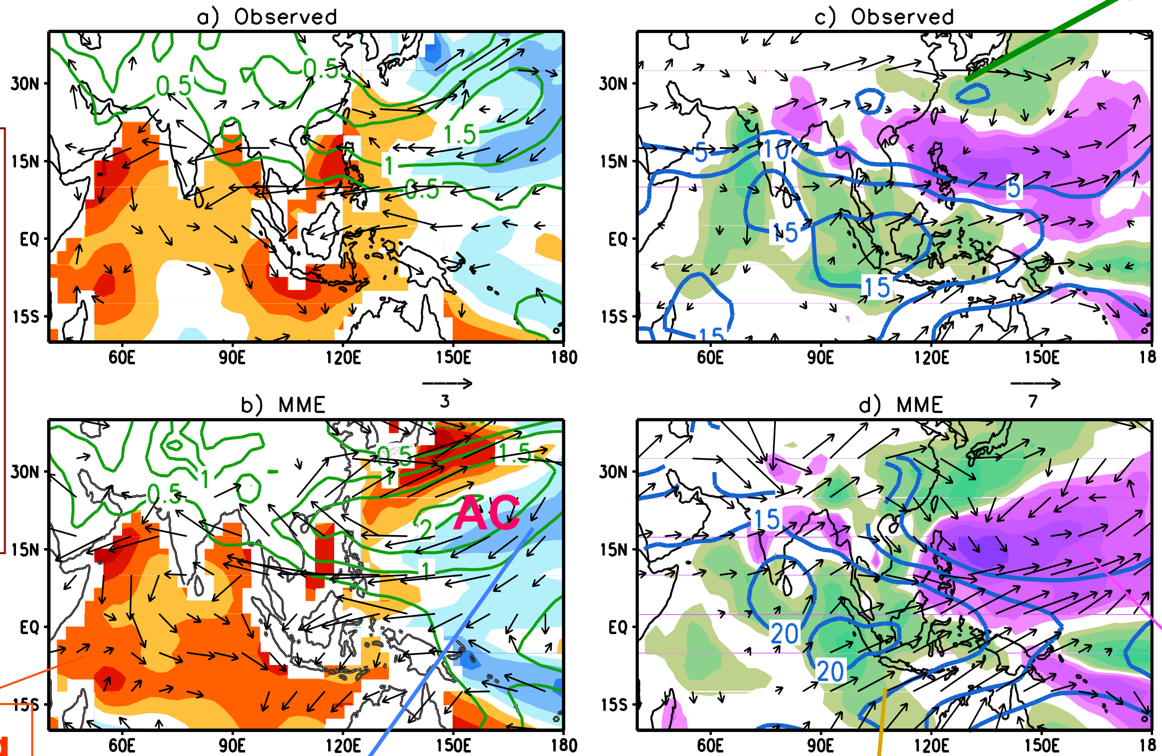

Precipitation (shaded) TT (contours), and 200hPa wind anomalies winds (vectors).

TIO warming

Suppressed rainfall

3. The subtropical westerly jet intensifies on the northern flank of the TT warming induced by the positive SST anomalies over the TIO. The intensified westerly jet could enhance atmospheric convection over the Meiyu/Baiu rain band by advecting warm temperature from the Tibetan plateau region (Sampe and Xie 2010). A surface circulation in response to enhanced Meiyu- Baiu convection would induce surface wind divergence in the subtropics and suppress convection there (Chowdary et al. 2010).

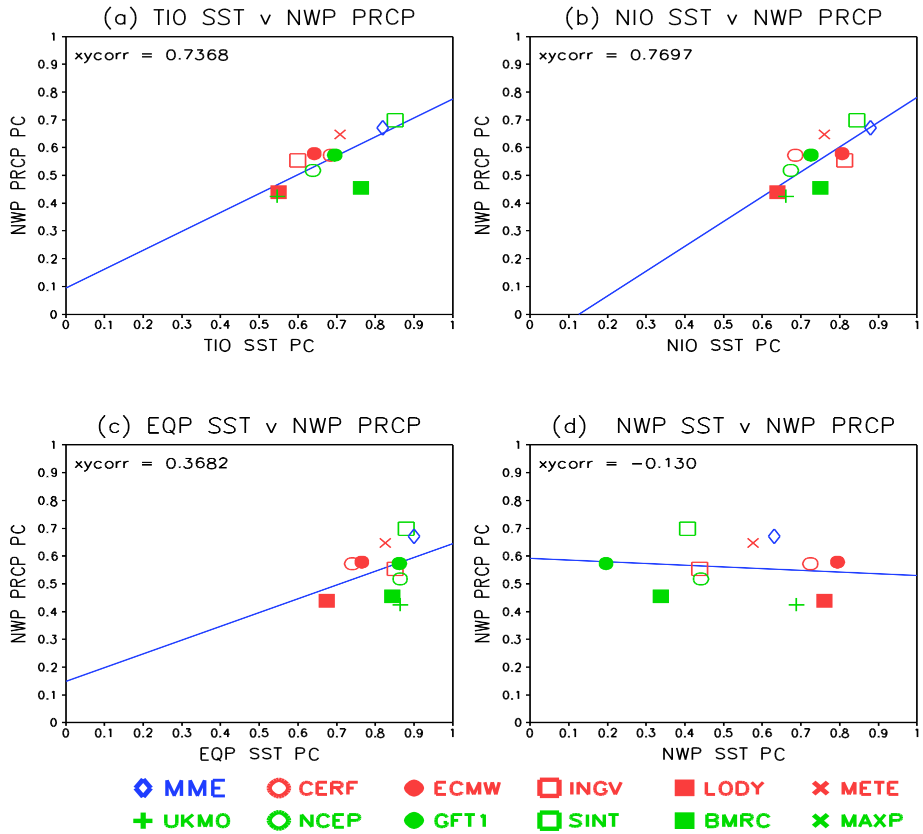

Scatter diagram between the forecast skill of JJA NW Pacific precipitation PC-2 and skills of regional SST PCs

(a) the TIO (20°S-20°N and 45ºE-100ºE)

(b) the NIO SST (0-20°N and 45ºE-100ºE)

(c) the equatorial Pacific (20ºS-20ºN and 120ºE-90ºW)

(d) the NW Pacific (0-40ºN and 120ºE-160ºE). All based on one-month lead forecast.

Strong correlation in skills between SST anomalies over TIO/NIO and NW Pacific rainfall predictability. Models that are skilful in capturing TIO/NIO SST anomalies are likely to be successful in predicting NW Pacific rainfall variability.

SINTEX Model no-TIO Experiment

The Scale Interaction Experiment (SINTEX) global ocean-atmosphere coupled GCM (Gualdi et al 2003) modified and improved at the Frontier Research Center for Global Change (SINTEX-F), Japan (Luo et al. 2005a, b, 2007, 2008).

The atmospheric component is the ECHAM 4.6 (Roeckner et al. 1996) with T106 spectral resolution and 19 vertical hybrid sigma-pressure levels. The oceanic component is OPA8.2 with 2° in longitude, latitudinal resolution increased to 0.5° within 2° of the equator. It has 31 layers in the vertical (Madec et al. 1998).

Nine-member ensemble retrospective forecasts for 12 target months from the first day of each month during 1983-2006 are performed. The 9 members are generated on the basis of three different coupling physics (i.e., three different models) with three different initial conditions for each model (Luo et al. 2007, 2008).

In the control run, the atmosphere and global ocean are fully interactive. An additional **TIO decoupled run** (NoTIO) is performed where the monthly mean climatology of Reynolds et al. (2002) SST is prescribed in the TIO between 25°S and 25°N.

The ocean model continues to respond to atmospheric variability, resulting in non-zero anomalies over the TIO. By decoupling the TIO, we aim to isolate its effect on climate elsewhere. Forecast anomaly is computed for each ensemble member relative to its own climatology.

SLP EOF

Observed | **CTL run (3-month lead)** | **NoTIO run (3-month lead)**

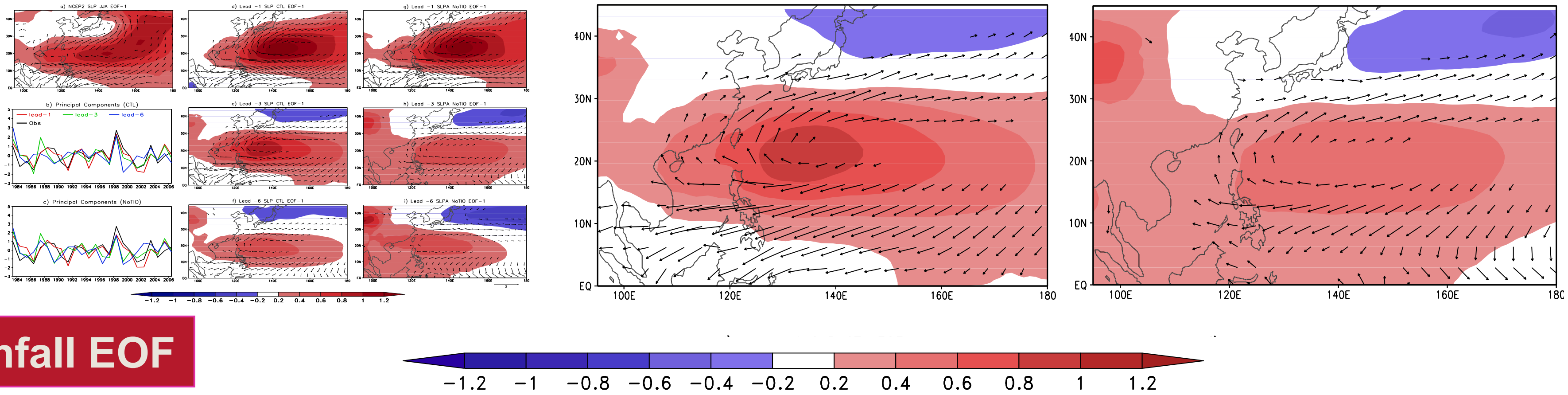

Rainfall EOF

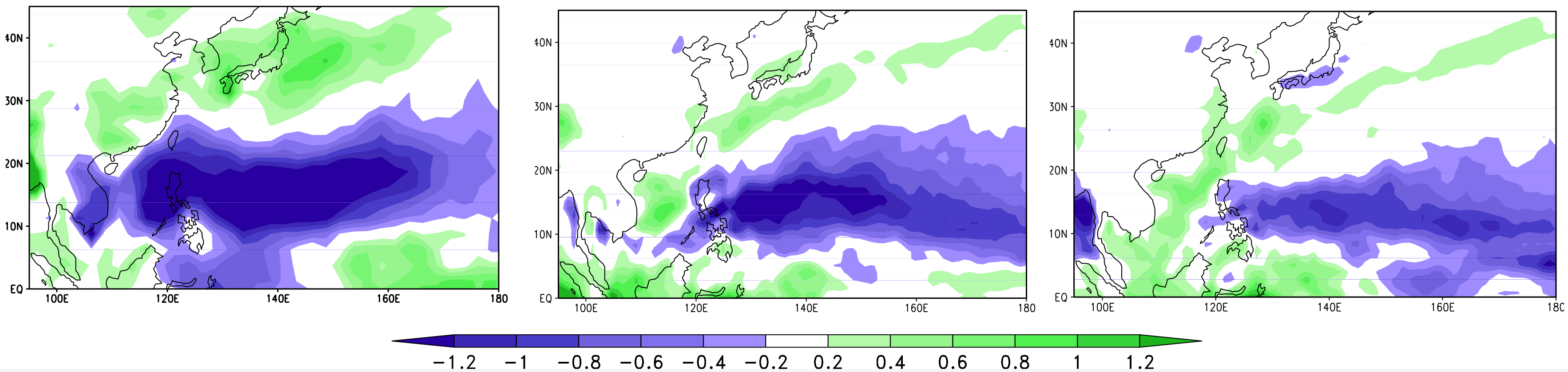

The model captures the subtropical SLP increase quite well up to 6-month lead while the anomaly magnitude decreases with lead time. Spatial patterns are better organized in the control than NoTIO run, especially for long lead predication.

The model captures this JJA(1) mode of precipitation in terms of spatial pattern except over Indochina Peninsular and the South China Sea where the model predicts a rainfall increase instead of an observed decrease.

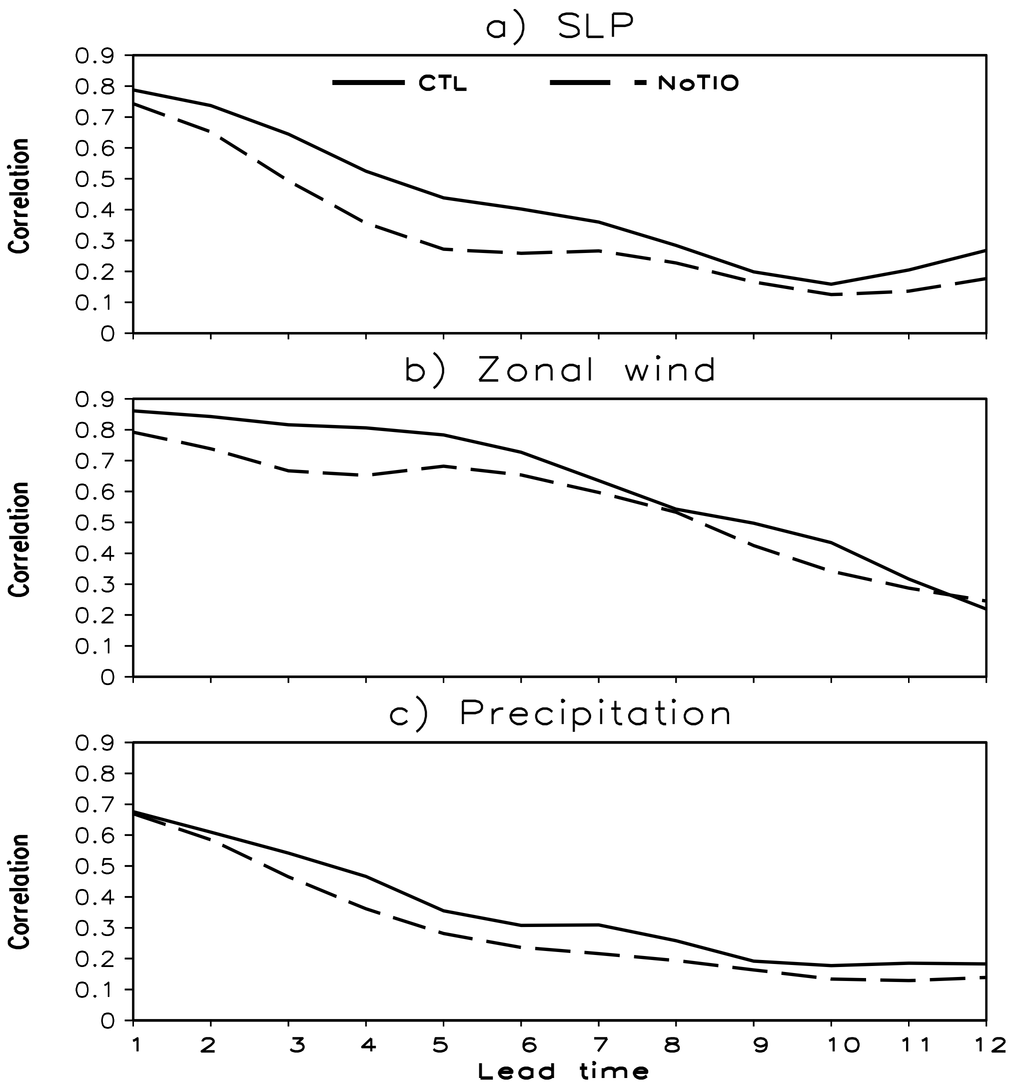

Chowdary et al. (2011) Clim. Dyn.

The ACC skill for SLP PC-1 decays with increasing lead but is significantly higher in the control than No-TIO run. At 4-month lead, ACC still exceeds 0.5 in the control but falls below 0.4 in the NoTIO run.

ACC remains high at 0.7 even at 6-month lead in the control (Fig. b), illustrating high prediction skills for the NW Pacific anticyclone.

The ACC remains about 0.5 at 4-month lead in the control but drops below 0.4 in the NoTIO run (Fig. c). In the NoTIO run, precipitation anomalies are generally weaker than in the control.

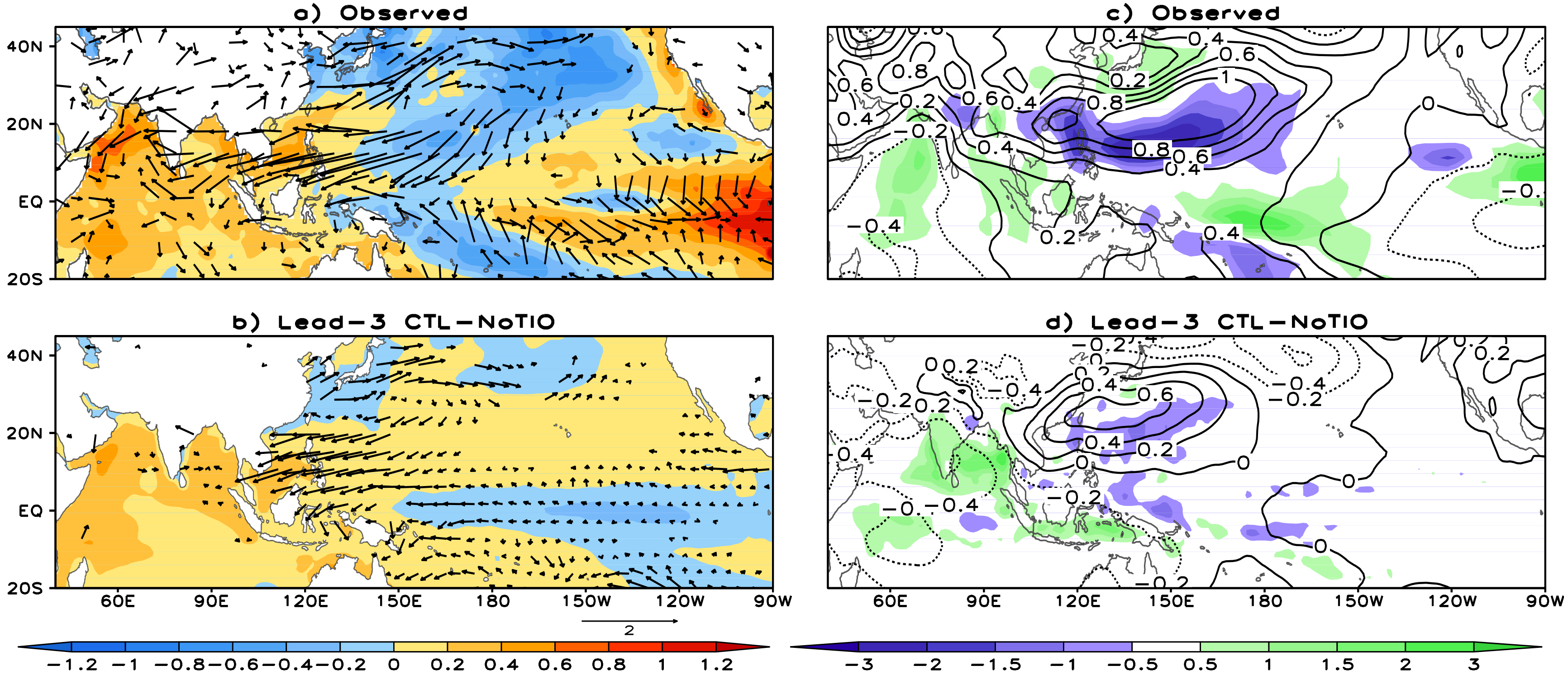

At lead 3, the control-NoTIO differences in SST, surface wind, SLP and precipitation are consistent with the Kelvin wave-induced Ekman divergence mechanism. (Xie et al. 2009; Chowdary et al. 2011)

Summary:

✓Analysis of multi-model hindcasts demonstrated that to predict NW Pacific atmospheric anomalies during JJA(1), our result show that models need to predict the TIO SST and precipitation well along with SST cooling on the south-eastern flank of anticyclone.

✓Couple model experiment result shows that an interactive TIO contributes to increasing the skill of atmospheric anomaly forecasts over the NW Pacific by as much as 50%.

✓Two mechanisms are identified for TIO to affect NW Pacific rainfall variability during JJA(1) remotely. One is the Kelvin wave- induced Ekman divergence mechanism [*Xie et al*., 2009] and the other is through intensifying the subtropical westerly jet [Chowdary et al., 2010).

Thank You

References

Chowdary, J. S., S.-P. Xie, H. Tokinaga, Y. M. Okumura, H. Kubota, N. C. Johnson, and X.-T. Zheng, 2012: Inter-decadal variations in ENSO teleconnection to the Indo-western Pacific for 1870-2007. *J. Climate*, 25, 1722-744.

Xie, S.-P., Y. Du, G. Huang, X.-T. Zheng, H. Tokinaga, K. Hu, and Q. Liu, 2010: Decadal shift in El Nino influences on Indo-western Pacific and East Asian climate in the 1970s. *J. Climate*, 23, 3352-3368.

Kosaka, Y., J. S. Chowdary, and S.-P. Xie, 2012: Limitations of seasonal predictability for summer climate over East Asia and the Northwestern Pacific. *J. Climate*, in press.

Chowdary, J. S., S.-P. Xie, J.-J. Luo, J. Hafner, S. Behera, Y. Masumoto, and T. Yamagata, 2011: Predictability of Northwest Pacific climate during summer and the role of the tropical Indian Ocean. *Clim. Dyn.*, 36, 607-621, doi:10.1007/s00382-009-0686-5.

Chowdary, J. S., S.-P. Xie, J.-Y. Lee, Y. Kosaka and B. Wang, 2010: Predictability of summer Northwest Pacific climate in eleven coupled model hindcasts: Local and remote forcing. *J. Geophys. Res.-Atmos.*, 115, D22121, doi:10.1029/2010JD014595.

Xie, S.-P., K. Hu, J. Hafner, H. Tokinaga, Y. Du, G. Huang, and T. Sampe, 2009: Indian Ocean capacitor effect on Indo-western Pacific climate during the summer following El Nino. *J. Climate*, 22, 730–747.

Huang, G., K. Hu, and S.-P. Xie, 2010: Strengthening of tropical Indian Ocean teleconnection to the Northwest Pacific since the mid-1970s: An atmospheric GCM study. *J. Climate*, 23, 5294-5304.

Watanabe, M., and F.-F. Jin, 2002: Role of Indian Ocean warming in the development of Philippine Sea anticyclone during ENSO. *Geophys. Res. Lett.*, **29,** 1478, doi:10.1029/2001GL014318.

Wang B, R Wu, and X. Fu, 2000: Pacific-East Asian teleconnection: How does ENSO affect east Asian climate?. *J. Climate,* **13,** 1517-1536.

Nitta, T., and S. Yamada, 1989: Recent warming of tropical sea surface temperature and its relationship to the Northern Hemisphere. *J. Meteor. Soc. Japan*, **67,** 375–383.

✓**NW Pacific low level circulation/rainfall is not correlated with local SST anomalies during summer.**

Pacific-Japan pattern

(Nitta 1986, 1987, JMSJ)

But what anchors it?

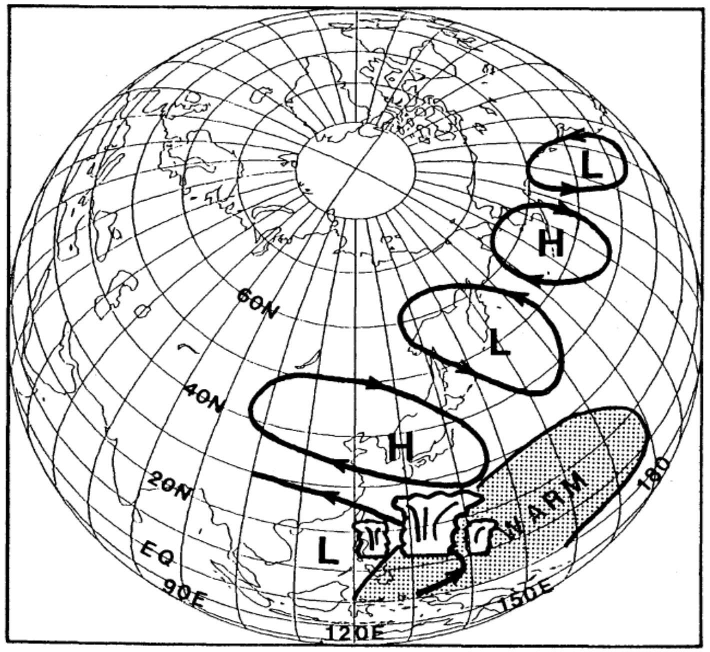

Fig. 18. Schematic pictures showing the relationships between SST anomalies, convective activities and atmospheric Rossby-wave trains.

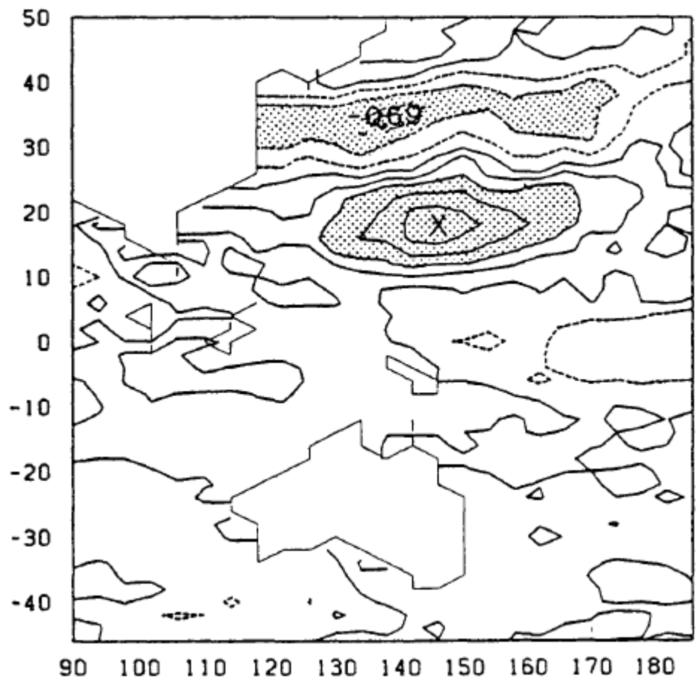

One point correlation with high cloud amount at 146E, 18N for 1978-83. Nitta (1986)

We have studied the centennial modulation of interannual variability over the Indo-western Pacific and its relationship to ENSO for 1870-2007 through the innovative use of surface meteorological observations along a busy ship track across the North Indian Ocean and South China Sea. Four epochs, 1883 to1909 (epoch-1), 1910 to 1936 (epoch-2), 1950 to 1976 (epoch-3) and 1977 to 2003 (epoch-4) are chosen based on the seasonal evolution of NIO SST warming associated with ENSO.

During the decades in the late 19th-early 20th century and in the late 20th century, the El Niño-induced NIO warming persists longer than during the 1910s-mid 1970s, well into the summer following the peak of El Niño. During the epochs of the prolonged NIO warming, rainfall drops and sea level pressure rises over the tropical Northwest Pacific in summer following El Niño. Conversely during the period when the NIO warming dissipates earlier, these atmospheric anomalies are not well developed. This supports the Indian Ocean capacitor concept as a mechanism prolonging El Niño influence into summer through the persistent Indian Ocean warming after El Niño itself has dissipated.

The decadal changes in ENSO teleconnection coincide with that of the PDO and IPO after the 1950s but this correlation breaks down prior to 1950s. Our results suggest that this decadal modulation of teleconnections associated with ENSO over the Indo-western Pacific is governed primarily by ENSO variance.

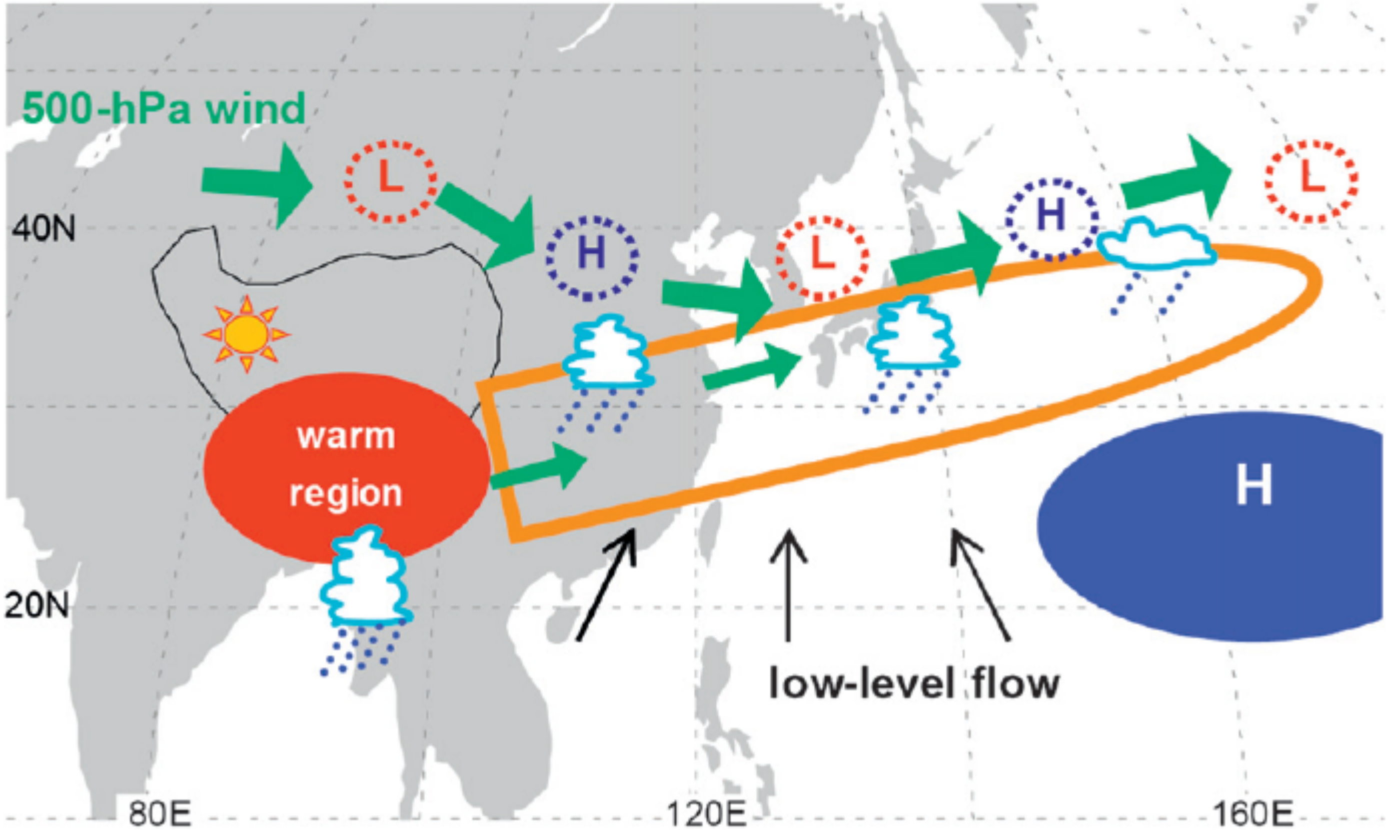
500-hPa wind
L
H
L
H
L
40N
20N
warm
region
H
low-level flow
80E
120E
160E

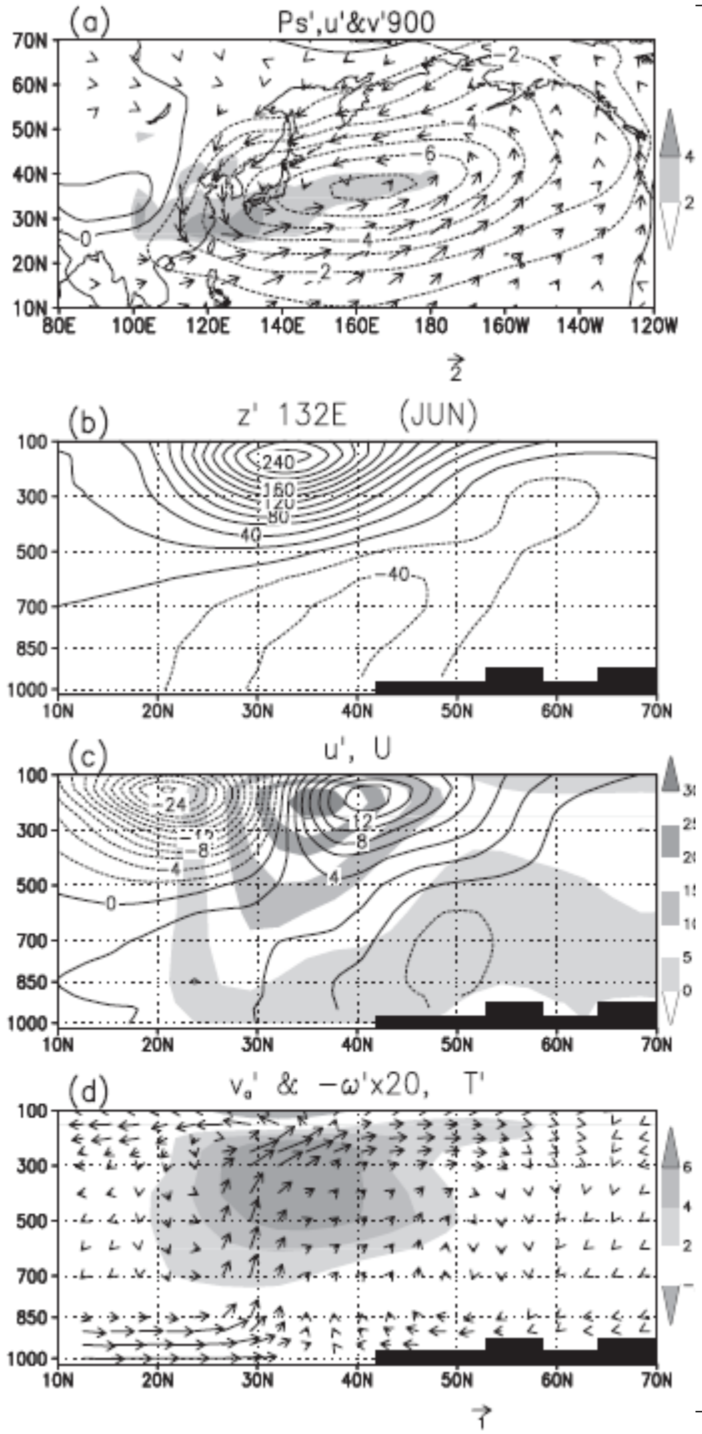

FIG. A1. LBM response to June heating of JRA-25 prescribed in the domain (258–508N, 1008E–1608W). (a) Surface pressure (contours at every 1 hPa), 900-hPa wind (arrows) and the prescribed heating at the 0.45 sigma level (shading, K day21). Meridional sections at 1328E: (b) geopotential height (contours at every 20 m); (c) zonal wind velocity (contours at every 2 m s21) overlaid on the basic-state zonal wind velocity (shading, m s21); (d) temperature (shading in K) with meridional and vertical components of ageostrophic wind (arrows in m s21 and Pa s21, respectively; vertical component is multiplied by 20).

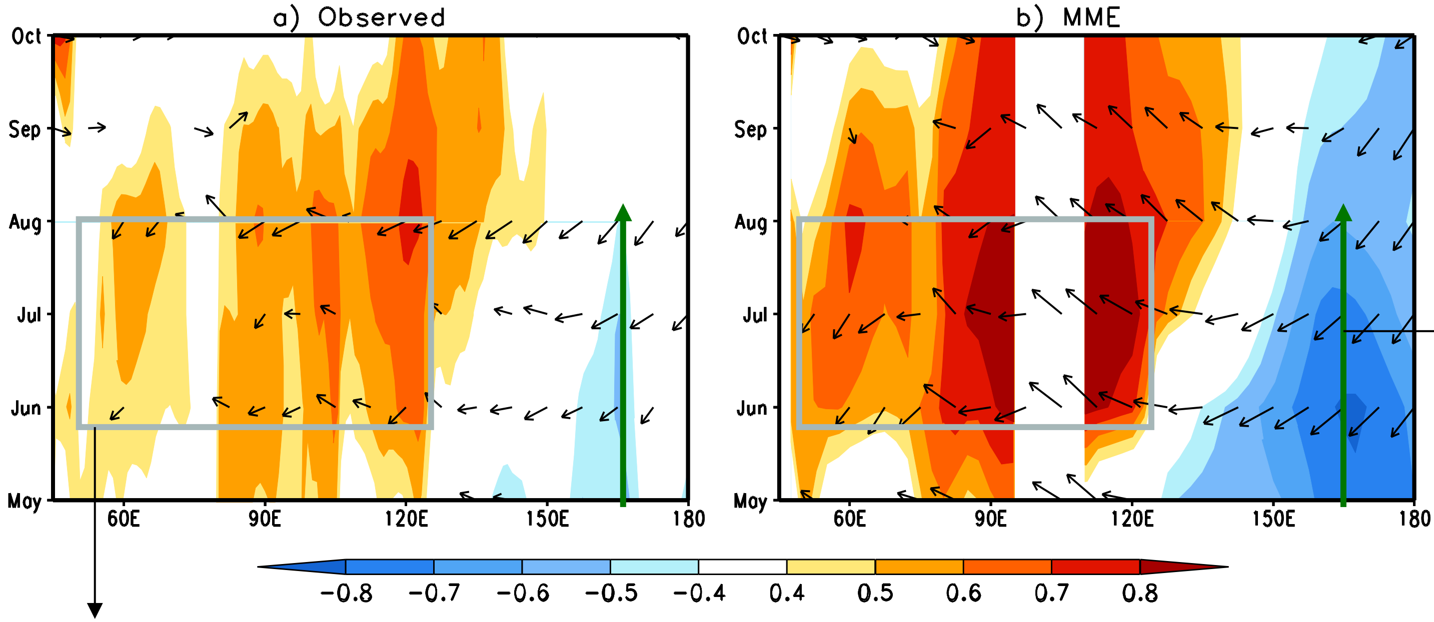

Decay cooling

TIO & SCS warming

Correlation of SST (Shaded) and 850hPa wind anomalies (vectors) averaged from 5ºN to 20ºN against the NW Pacific SLP PC-1: (a) observations, (b) MME initialized on 01May. Y-axis is calendar month during decay phase of El Niño.